Ecotones and LiDAR in tropical dry forests

by

Menglei Duan

A thesis submitted in partial fulfillment of the requirements for the degree of

Master of Science

Department of Earth and Atmospheric Sciences
University of Alberta

Abstract

Secondary succession is defined as natural regeneration following complete forest clearance from anthropogenic or natural disturbances. Traditional strategies aimed to map and characterize secondary succession using remote sensing are usually based on deterministic approaches, where transitions between successional stages are not considered. These transitions represent rich environments between successional stages and play a key role in ecosystem regeneration. Here, we evaluate the use of the Full-waveform Airborne LiDAR to characterize changes in forest structure between the transition of early-to-intermediate and intermediate-to-late forest succession at the Santa Rosa National Park Environmental Monitoring Super Site (SRNP-EMSS), Guanacaste, Costa Rica. The vertical forest structure was analyzed on twenty cross-sections selected between forest transitions previously mapped using machine learning; leaf area density (LAD) and waveform metrics were studied based on the waveform profile derived from twenty-seven plots distributed in different successional forest patches. Results suggest that LiDAR techniques can identify forest structure differences between successional stages and their transitions. The significance proves that transitions exist, highlights the unique transitional characteristics between intermediate and late successional stages and contributes to understanding the significance of inter-successional stages (transitions) in secondary dry forests.

Keywords: Tropical Dry Forests (TDFs); ecological succession; forest structure; transition; full-waveform LiDAR; cross-sections; shape-based metrics.

Preface

This thesis is an original work by Menglei Duan. Chapter 2 “Characterizing Transitions between Successional Stages in a Tropical Dry Forest Using LiDAR Techniques” was published in Remote Sensing (https://doi.org/10.3390/rs15020479).

Acknowledgements

I would like to thank my supervisor Dr. Arturo Sanchez-Azofeifa for the honor of being a member of the Centre for Earth Observation Sciences (CEOS) at the University of Alberta. Thank you for your constant support and guidance during my master's study.

I extend my gratitude to my committee members, Dr. Benoit Rivard and Dr. Kati Laakso, for their comments to improve my research. I also thank Dr. Michael Hesketh for his help and coordination in the lab.

Many special thanks to all my colleagues in the CEOS lab: Connor Bax, Nooshin Mashhadi, Steven Wagers, Patrick O'Brien, Dr. Tao Han, Andre Truksa, Paula Moreno Pina, Ronny Alexander Hernandez Mora, Mohammed Abdaki, Xinyu Lei, Gaili He, and Chenzherui Liu. I am so happy to meet such close friends in Canada. We have numerous good memories, and I retreat these experiences as a precious fortune in my life.

I sincerely thank the friends I met in El Cortez, a Mexican kitchen where I worked part-time: Karla, Jahir, Aniris, Dylan, Randy, Rocio, Gabriela, Abuma, Amy, Patrick, Nestor, Obi, Octavio, Kae, Michelle, and Jana. I truly enjoyed the time we worked and talked together. This experience totally enriches my life when I am away from school.

Furthermore, I would like to thank my girlfriend Xiaofan Yu for her company. Most importantly, I express my gratefulness to my family for their unconditional support, help and encouragement in my life.

Table of Contents

1. Chapter 1: Introduction 1

1.1 References 7

2. Chapter 2: Characterizing Transitions between Successional Stages in a Tropical Dry Forest using LiDAR Techniques 14

2.1 Introduction 14

2.2 Materials and Methods 18

2.2.1 Study Area 18

2.2.2 Data Acquisition 19

2.2.2.1 Forest cover map 19

2.2.2.2 Full-waveform LiDAR 20

2.2.3 Data Processing 20

2.2.3.1 Transition identification 20

2.2.3.2 Estimation of canopy height variation 21

2.2.3.3 Canopy height comparison between transitions and main successional stages 22

2.2.3.4 Estimation of vertical forest structure 22

2.2.3.5 Derivation of LiDAR metrics 24

2.3 Results 26

2.3.1 Transitions 26

2.3.2 Changes in canopy height across transitions 26

2.3.3 Forest structure characteristics of transitions 27

2.4 Discussion 29

2.5 Conclusions 34

2.6 References 35

2.7 Tables 42

2.8 Figures 46

3. Chapter 3: Conclusions 55

3.1 Synthesis of significant contributions 55

3.2 Future work and challenge 56

3.3 References 58

Bibliography 59

List of Tables

Table 1. Technical specifications of the flight parameters and sensors of the study. Data were acquired in the SRNP-EMSS on May 21, 2021. Abbreviations: GSD=ground sampling distance, FOV=field of view. 42

Table 2. LiDAR metrics are used to characterize a waveform as a function of the successional stage (after Gu et al. (2018)). 43

Table 3. Mean values with one standard deviation of canopy height with three successional stages and two transitions at the SRNP-EMSS were extracted from LiDAR data. Significant differences (F values) according to the successional stages are presented from ANOVA. Height was extracted in meters and tree individuals per stage. 44

Table 4. Mean (±SD) of metrics derived from the full-waveform LiDAR along the nine cross-sections over two successional stages and one transition in the dry forest at the SRNP-EMSS, Guanacaste, Costa Rica. Significant differences (F values) according to different successional stages are provided. C_x, the x coordinate of the waveform centroid; C_y, the y coordinate of the waveform centroid; RG, the radius of gyration; P_x, the x coordinate of the maximum waveform amplitude; P_y, the y coordinate of the maximum waveform amplitude; H_{max}, maximum tree height (m); LAI, leaf area index. 45

List of Figures

Figure 1. The traditional and refined principles for mapping secondary TDFs succession. (a) Traditional definitions assume that different successional stages (1, 2 and 3) have deterministic extents. (b) Approaches considering the presence of transitions (such as 2 and 4) between the principal successional stages 1, 3 and 5. 46

Figure 2. The study area at the Santa Rosa National Park Environmental Monitoring Super Site (SRNP-EMSS), Guanacaste, Costa Rica (a), the forest cover map from Zhao et al. (2021) generated with LVIS and HyMap data in (b), Riegl Full-waveform Airborne LiDAR data 2021, acquired in SRNP-EMSS (c), the datasets from subfigures b and c overlain on top of each other to define the study area. 47

Figure 3. A canopy height model with a 5m*5m spatial resolution and the spatial distribution of five successional stages at the SRNP-EMSS, Guanacaste, Costa Rica. The range is the overlapping between the forest cover map (Zhao et al., 2021) and full-waveform LiDAR data (Figure 2. (d)). Twenty cross-sections (black lines) of 500 meters in length and twenty-seven plots (nine for each successional stage) with an area of 45m*45m along the successional gradient were extracted randomly and evenly over the study area. 48

Figure 4. The figure describes the centroid (C_x and C_y), the radius of gyration (RG), and the coordinate of maximum waveform amplitude (P_x and P_y) based on the LAD profile waveform (after Muss et al. (2013)). 49

Figure 5. Transitions extracted by building a 25m-buffer from the forest age map, which was defined into three principal successional stages according to age (Zhao et al., 2021). To improve the accuracy and reasonability of transition zone extraction, some forest patches with small areas (< 5000 m^2 in early, < 10000 m^2 in intermediate, and < 2000 m^2 in late) were dropped (i.e., white dots represent data gaps and strips represent invalid noise). Figures (a) and (b) are an example and zoom-in views of a selected transition zone at the SRNP-EMSS, Guanacaste, Costa Rica. 50

Figure 6. Canopy height variability of successional stages at the SRNP-EMSS, Guanacaste, Costa Rica, derived from a Canopy Height Model (CHM) over Early, Transition I: Early to Intermediate, Intermediate, Transition II: Intermediate to Late, and Late successional stages. 51

Figure 7. Twenty profiles were derived from randomly selected cross-sections along the path of succession at the SRNP-EMSS (Figure 3). The x-axis is the

distance along the profile (i.e., 0 — 500m). The y-axis is canopy height in meters (the range: 0 — 35m). Transition II (from Intermediate to Late successional stage) is highlighted in light blue. (a) — (g) describe the change of canopy height along the Late — Transition II— Intermediate — Transition II— Late; (h) describes the change of canopy height along the Intermediate — Transition II— Late — Transition II— Intermediate; (i) — (j) describe the change of canopy height along the Intermediate — Transition II— Intermediate; (k) — (t) describe the change of canopy height along the Intermediate — Transition II— Late (All transitions refer to the successional stage from intermediate to late). The solid red line represents a fitted smooth change trend. 52

Figure 8. The vertical LAD profile of the nine plots for the Intermediate (a), Transition II(b), and Late successional stage (c). The solid red line in each subfigure is the average for the corresponding nine waveforms. 53

Figure 9. Violin plots for the LiDAR metrics (C_x, C_y, P_x and P_y) distribution along the forest successional gradients (Intermediate — Transition II— Late) from 27 plots at the SRNP-EMSS, Guanacaste, Costa Rica. C_x, the x coordinate of the waveform centroid; C_y, the y coordinate of the waveform centroid; P_x, the x coordinate of the maximum waveform amplitude; P_y, the y coordinate of the maximum waveform amplitude. 53

Figure 10. A scatter plot of RG (the radius of gyration) versus LAD (Leaf Area Density) for three successional gradients (Intermediate, Transition II and Late) from 27 plots at the SRNP-EMSS, Guanacaste, Costa Rica. 54

List of Symbols

TDFs	Tropical Dry Forests
LiDAR	Light Detecting and Ranging
DR LiDAR	Discrete LiDAR
FW LiDAR	Full-waveform LiDAR
ALS	Airborne Laser Scanning
TLS	Terrestrial Laser Scanner
SRNP-EMSS	Santa Rosa National Park Environmental Monitoring Super Site
GSD	Ground sampling distance
FOV	Field of view
LVIS	Land Vegetation and Ice Sensor
SLICER	The Scanning LiDAR Imager of Canopies by Echo Recovery
GLAS	The Geoscience Laser Altimeter System
CHM	Canopy Height Model
LAI	Leaf Area Index
LAD	Leaf Area Density
AGB	Aboveground Biomass
PAR	Photosynthetically active radiation
$\mathbf{C_x}$	The x coordinate of the centroid

C_y	The y coordinate of the centroid
P_x	The x coordinate of the maximum waveform amplitude
P_y	The y coordinate of the maximum waveform amplitude
RG	The radius of gyration
RNAA	Randomized Nonlinear Archetypal Analysis
CSF	The “cloth” simulation filter
LMF	Local Maximum Filter
IDW	Inverse distance weighted
ANOVA	A univariate analysis of variance

1. Chapter 1: Introduction

The rate of ecosystem loss has increased significantly in the last half of the 20th century (Houghton et al., 1991) due to demographic growth, economic booms, agricultural and colonization policies, and external factors (Barbier, 2004; Houghton et al., 1991; Marquette, 2006). Tropical Dry Forests (TDFs) are an important component of the global ecosystem and play a crucial role in ecosystem services, including biodiversity conservation, water conservation, and global climate regulation (Janzen, 1986). TDFs are considered one of the most threatened ecosystems on Earth, although they account for about 46% of tropical forests (Cao et al., 2015; Olson et al., 2001).

Sánchez-Azofeifa et al. (2005) described TDFs as a vegetation type typically dominated by deciduous trees, with more than half of them are drought deciduous. The mean annual temperature is > 25 °C , total annual precipitation ranges from 700 to 2000mm, and have three or more months every year with precipitation < 100mm. Up to now, TDFs landscapes are a combination of different land-use and land-cover classes for the purpose of implementing of conservation and management programs (Cao et al., 2015; Li et al., 2017). Savannas, coastlines, mangroves and gallery forests are associated vegetation types within the TDF matrix (Sánchez-Azofeifa et al., 2005). A distinguishing characteristic of TDFs is that the most species-rich areas are also among the driest (Kalacska et al., 2004). For instance, studies in Chamela, Mexico and Bolivia have a greater diversity than those in Guanacaste, Costa Rica with more precipitation (Portillo-Quintero and Sánchez-Azofeifa, 2010). Moreover, another feature of TDFs is that they defy the well-established trend of increasing species

richness as one approaches the equator (Gentry, 1988). The most diverse neotropical tropical dry forests are the farthest from the equator in Mexico and South America (Argentina, Brazil, Bolivia and Paraguay) (Kalacska et al., 2004).

Ecological mechanisms related to secondary TDFs regeneration after land abandonment have been widely studied over recent decades (Aide et al., 1996; Khurana and Singh, 2001). Secondary TDF succession is affected by soil, topography, land-use history, and propagule availability (Arroyo-Mora et al., 2005). As a result, TDFs in different successional stages show differences in the forest's vertical and horizontal structure, species composition, leaf flushing dynamics, and the density of green canopy cover (Li et al., 2017). Based on these differences, TDFs regeneration processes are generally divided into early, intermediate, and late along an ecological gradient (Arroyo-Mora et al., 2005; Cao et al., 2015; Kalacska et al., 2004).

One of the major problems associated with the study of ecological succession in TDFs is the lack of information that is present between different successional stages. Ecological regeneration is an ongoing process, as a result, transitions between principal successions have become an important contribution to the landscape. Some scholars named it as ecotones. Natural ecotones are valuable habitats for biodiversity and protect the interior of forests (Czaja et al., 2021). Ecotone zones are still insufficiently understood in ecology.

Forest structure is defined as the bottom to the top configuration of above-ground vegetation within a forest stand (Latifi, 2009). TDFs forest structure studies have successfully characterized forest structure and its temporal changes in early, intermediate and late successional stages (Cao et al., 2015; Castillo et al., 2012; Gu et al., 2018; Kalacska et al., 2004). These studies have found that early successional

stages have lower biomass and simple vegetation structures and are dominated by small trees, shrubs, and pastures. The intermediate successional stages have more biomass and mixed species from the early and late stages; trees with bigger and denser canopies dominate this successional stage. Late successional stages are characterized by the highest species diversity and more considerable variability in canopy openness; moreover, trees are infested with lianas (Sánchez-Azofeifa et al., 2017). In other words, the successional sequence observed is related to changes in the vertical distribution of woody components that occur when forest patches evolve from an early stage dominated by sparse trees and grass, to an intermediate stage characterized by small canopies and a high density of understory regeneration, and then to more complex and developed stages of intermediate and late stage secondary succession which share some attributes of old growth forests (Castillo et al., 2012). Despite the importance of these studies, a key denominator is that they did not identify relevant forest structural attributes for inter-successional stages or transitions. These transitions represent slight variability and unique forest structural characteristics during the ecological succession process, compared with the main successional stages.

The use of passive optical sensors dominates traditional remote sensing applications in TDFs. Early studies have succeeded in characterizing forest attributes (Arroyo-Mora et al., 2005; Kalacska et al., 2005; Kalácska et al., 2005) through linking spectral reflectance or vegetation indices with specific forest structural parameters. More recently, Light Detection and Ranging (LiDAR) has shown the superiority in the study of TDFs succession and forest structure (Castillo et al., 2012) . Based on the recording mode, LiDAR systems are characterized into discrete return (DR) and full waveform (FW). The DR LiDAR systems generally have a small footprint (less than 1m), and record multiple returns per laser pulse (Gu et al., 2018). They have been

widely used to estimate forest stand variables (Clark et al., 2004; Drake et al., 2002), canopy gap probability (Lovell et al., 2003), aboveground biomass (AGB) (Skowronski et al., 2014; Zhao et al., 2009) and vertical forest structure. However, the DR LiDAR systems suffer from several drawbacks, especially the limited number of returns, which means they can hardly derive repeatable relationships between field and LiDAR estimations of forest structure (Armston et al., 2013). In contrast, the FW LiDAR systems have historically been large-footprint (10-70m diameter). Large-footprint FW LiDAR systems can derive a continuous waveform of the signal return so that we can acquire the complete signal emitted by the sensor as opposed to discrete hits (Crespo-Peremarch et al., 2020); more importantly, they have wide spatial coverage. In this case, data can be processed as a continuous return signal providing abundant reliable information within the forest's vertical components. Several classic large-footprint LiDAR systems have been applied widely in forestry within decades, such as the Land Vegetation and Ice Sensor (LVIS) system (Blair et al., 1999), the Scanning LiDAR Imager of Canopies by Echo Recovery (SLICER) onboard aircraft, and the Geoscience Laser Altimeter System (GLAS) onboard satellite (Abshire et al., 2005). In addition, most commercial FW LiDAR systems are small-footprint (0.2-3m diameter), depending on flying height and beam divergence with higher repetition frequency. They provide a high point density and an accurate altimetric description within the diffraction cone (Mallet and Bretar, 2009).

Several previous studies have tried to study TDFs and ecological succession using FW airborne LiDAR (Castillo et al., 2012; Li et al., 2017;Gu et al., 2018; Zhao et al., 2021). Castillo et al. (2012) identified successional stages at a TDF site in Costa Rica using a LVIS dataset. Their findings show that LIDAR data can identify three successional subclasses within the intermediate stage providing further insights into

the development of secondary forest growth. Li et al. (2017) explored transition zones between different types of intermediate secondary TDFs using a LVIS dataset and hyperspectral remote sensing images. However, they did not characterize the forest structure of these transition zones. Gu et al. (2018) extracted different LiDAR metrics based on the LVIS dataset to quantify forest structure as a function of different levels of ecological succession. Particularly, they proved the shape-based LiDAR metrics can be used in the study of ecological succession and forest structure. More recently, Zhao et al. (2021) investigated the potential of multi-source, full-waveform LiDAR and hyperspectral remote sensing data fusion for the evaluation of the forest age.

The overall objective of this thesis is to explore forest structure changes along the successional path using LiDAR techniques at a TDF site in Costa Rica. Two datasets were used in this study: (1) a forest cover map derived from Zhao et al. (2021); (2) a small-footprint FW LiDAR data collected by Stereocarto (Madrid, Spain) in 2021. Particularly, this study highlights the unique forest structure feature of TDFs transitions (i.e., from early to intermediate and from intermediate to late). To this end, Chapter 2 aims to achieve the goals of this thesis.

Chapter 2. "Characterizing Transitions between Successional Stages in a Tropical Dry Forest (TDF) using LiDAR Techniques" explores forest structure along the successional path. Here I identified transition zones based on Zhao et al. (2021) by building a buffer between each main successional stage. Once the known transition regions were identified, I used a colorized small footprint full-waveform airborne LiDAR dataset to create the Canopy Height Model. Then twenty 500m transects between intermediate and late forests, as well as their transitions were randomly selected over the study area to quantify canopy height changes. On the other hand, twenty-seven plots in different successional stages (intermediate, transition II, and

late) were picked to characterize vertical structure differences. I derived each plot's the leaf area density (LAD) profile and calculated different metrics from the corresponding vertical profile waveform. The rest of the results and analysis will be addressed within the Result and Discussion section of Chapter 2.

Finally, Chapter 3, "Conclusions," summarizes the significant findings related to TDFs' inter-successional stages and corresponding forest structure characteristics. In addition, this section also points out the limitation of the method I used and potential future work based on this study.

1.1 References

Abshire, J.B., Sun, X., Riris, H., Sirota, J.M., Mcgarry, J.F., Palm, S., Yi, D., Liiva, P., 2005. Geoscience Laser Altimeter System (GLAS) on the ICESat Mission : On-orbit measurement performance 32, 11–14. https://doi.org/10.1029/2005GL024028

Aide, M., Zimmerman, J., Rosario, M., Marcano, H., 1996. Forest Recovery in Abandoned Cattle Pastures Along an Elevational Gradient in Northeastern Puerto Rico Author (s): T . Mitchell Aide , Jess K . Zimmerman , Maydee Rosario and Humfredo Marcano Source : Biotropica , Vol . 28 , No . 4 , Part A . Special Is. Biotropica 28, 537–548.

Armston, J., Disney, M., Lewis, P., Scarth, P., Phinn, S., Lucas, R., Bunting, P., Goodwin, N., 2013. Remote Sensing of Environment Direct retrieval of canopy gap probability using airborne waveform lidar. Remote Sens. Environ. 134, 24–38. https://doi.org/10.1016/j.rse.2013.02.021

Arroyo-Mora, J.P., Sánchez-Azofeifa, G.A., Kalacska, M., Rivard, B., Calvo-Alvarado, J.C., Janzen, D.H., 2005. Secondary Forest Detection in a Neotropical Dry Forest Landscape Using Landsat 7 ETM + and IKONOS Imagery Published by : Association for Tropical Biology and Conservation Stable URL : https://www.jstor.org/stable/30043218 REFERENCES Linked references are. Biotropica 37, 497–507.

Bagaram, M.B., Giuliarelli, D., Chirici, G., Giannetti, F., Barbati, A., 2018. UAV remote sensing for biodiversity monitoring: Are forest canopy gaps good covariates? Remote Sens. 10, 1–28. https://doi.org/10.3390/rs10091397

Barbier, E.B., 2004. Agricultural expansion, resource booms and growth in Latin America: Implications for long-run economic development. World Dev. 32, 137–157. https://doi.org/10.1016/j.worlddev.2003.07.005

Blair, J.B., Rabine, D.L., Hofton, M.A., 1999. The Laser Vegetation Imaging Sensor : a medium-altitude , digitisation-only , airborne laser altimeter for mapping vegetation and topography 115–122.

Bottalico, F., Chirici, G., Giannini, R., Mele, S., Mura, M., Puxeddu, M., Mcroberts, R.E., Valbuena, R., Travaglini, D., 2017. International Journal of Applied Earth Observation and Geoinformation Modeling Mediterranean forest structure using airborne laser scanning data. Int. J. Appl. Earth Obs. Geoinf. 57, 145–153. https://doi.org/10.1016/j.jag.2016.12.013

Bouvier, M., Durrieu, S., Fournier, R.A., Renaud, J., 2015. Remote Sensing of Environment Generalizing predictive models of forest inventory attributes using an area-based approach with airborne LiDAR data. Remote Sens. Environ. 156, 322–334. https://doi.org/10.1016/j.rse.2014.10.004

Burrough, P.A., 2001. GIS and geostatistics: Essential partners for spatial analysis. Environ. Ecol. Stat. 8, 361–377. https://doi.org/10.1023/A:1012734519752

Calvo-Rodriguez, S., Sanchez-Azofeifa, A.G., Duran, S.M., Espírito-Santo, M.M., 2016. Assessing ecosystem services in Neotropical dry forests: A systematic review. Environ. Conserv. https://doi.org/10.1017/S0376892916000400

Cao, S., Yu, Q., Sanchez-Azofeifa, A., Feng, J., Rivard, B., Gu, Z., 2015. Mapping tropical dry forest succession using multiple criteria spectral mixture analysis. ISPRS J. Photogramm. Remote Sens. 109, 17–29. https://doi.org/10.1016/j.isprsjprs.2015.08.009

Castillo-Núñez, M., Sánchez-Azofeifa, G.A., Croitoru, A., Rivard, B., Calvo-Alvarado, J., Dubayah, R.O., 2011. Delineation of secondary succession mechanisms for tropical dry forests using LiDAR. Remote Sens. Environ. 115, 2217–2231. https://doi.org/10.1016/j.rse.2011.04.020

Castillo, M., Rivard, B., Sánchez-Azofeifa, A., Calvo-Alvarado, J., Dubayah, R., 2012. LIDAR remote sensing for secondary Tropical Dry Forest identification. Remote Sens. Environ. 121, 132–143. https://doi.org/10.1016/j.rse.2012.01.012

Clark, M.L., Clark, D.B., Roberts, D.A., 2004. Small-footprint lidar estimation of sub-canopy elevation and tree height in a tropical rain forest landscape. Remote Sens. Environ. 91, 68–89. https://doi.org/10.1016/j.rse.2004.02.008

Crespo-peremarch, P., Ángel, L., Balaguer-beser, Á., Estornell, J., Cartography, G., Sensing, R., Cgat, G., València, U.P. De, Vera, C. De, 2018. ISPRS Journal of

Photogrammetry and Remote Sensing Analyzing the role of pulse density and voxelization parameters on full- waveform LiDAR-derived metrics. ISPRS J. Photogramm. Remote Sens. 146, 453–464. https://doi.org/10.1016/j.isprsjprs.2018.10.012

Crespo-Peremarch, P., Fournier, R.A., Nguyen, V.T., van Lier, O.R., Ruiz, L.Á., 2020. A comparative assessment of the vertical distribution of forest components using full-waveform airborne, discrete airborne and discrete terrestrial laser scanning data. For. Ecol. Manage. 473, 118268. https://doi.org/10.1016/j.foreco.2020.118268

Czaja, J., Wilczek, Z., Chmura, D., 2021. Shaping the ecotone zone in forest communities that are adjacent to expressway roads. Forests 12, 1–13. https://doi.org/10.3390/f12111490

Drake, J.B., Dubayah, R.O., Clark, D.B., Knox, R.G., Blair, J.B., Hofton, M.A., Chazdon, R.L., Weishampel, J.F., Prince, S.D., 2002. Estimation of tropical forest structural characteristics using large-footprint lidar. Remote Sens. Environ. 79, 305–319. https://doi.org/https://doi.org/10.1016/S0034-4257(01)00281-4

Gentry, A., 1988. Volume 75 Annals Number 1 of the Botanical Garden. Ann. Missouri Bot. Gard. 75, 1–34.

Gu, Z., Cao, S., Sanchez-Azofeifa, G.A., 2018. Using LiDAR waveform metrics to describe and identify successional stages of tropical dry forests. Int. J. Appl. Earth Obs. Geoinf. 73, 482–492. https://doi.org/10.1016/j.jag.2018.07.010

Hoekstra, J.M., Boucher, T.M., Ricketts, T.H., Roberts, C., 2005. Confronting a biome crisis: Global disparities of habitat loss and protection. Ecol. Lett. 8, 23–29. https://doi.org/10.1111/j.1461-0248.2004.00686.x

Houghton, R.A., Skole, D.L., Lefkowitz, D.S., 1991. Changes in the landscape of Latin America between 1850 and 1985 II. Net release of CO2 to the atmosphere. For. Ecol. Manage. 38, 173–199. https://doi.org/10.1016/0378-1127(91)90141-H

Janzen, D.H., 1986. The Future of Tropical Ecology Author (s): Daniel H . Janzen Source : Annual Review of Ecology and Systematics , Vol . 17 (1986), pp . 305-324 Published by : Annual Reviews Stable URL :

http://www.jstor.org/stable/2096998 THE FUTURE OF TROPICAL ECOLOG. For. Ecol. Manage. 17, 305–324.

Kalácska, M., Calvo-Alvarado, J.C., Sánchez-Azofeifa, G.A., 2005. Calibration and assessment of seasonal changes in leaf area index of a tropical dry forest in different stages of succession. Tree Physiol. 25, 733–744. https://doi.org/10.1093/treephys/25.6.733

Kalacska, M., Member, S., Sanchez-azofeifa, G.A., Caelli, T., Rivard, B., Boerlage, B., 2005. Using Bayesian Networks. IEEE Trans. Geosci. Remote Sens. 43, 1866–1873. https://doi.org/https://doi.org/10.1109/TGRS.2005.848412

Kalacska, M., Sanchez-Azofeifa, G.A., Calvo-Alvarado, J.C., Quesada, M., Rivard, B., Janzen, D.H., 2004. Species composition, similarity and diversity in three successional stages of a seasonally dry tropical forest. For. Ecol. Manage. 200, 227–247. https://doi.org/10.1016/j.foreco.2004.07.001

Kalacska, M., Sanchez-azofeifa, G.A., Rivard, B., Caelli, T., 2007. Ecological fingerprinting of ecosystem succession : Estimating secondary tropical dry forest structure and diversity using imaging spectroscopy. Remote Sens. Environ. 108, 82–96. https://doi.org/10.1016/j.rse.2006.11.007

Khurana, E., Singh, J.S., 2001. Ecology of seed and seedling growth for conservation and restoration of tropical dry forest : A review. Environ. Conserv. 28, 39–52. https://doi.org/10.1017/S0376892901000042

Latifi, H., 2009. Characterizing Forest Structure by Means of Remote Sensing : A Review.

Leafsky, M.A.., Cohen, W.B.., Parker, G.G.., Harding, D.J., 2002. Lidar Remote Sensing for Ecosystem Studies. Bioscience 52, 19–30. https://doi.org/https://doi.org/10.1641/0006-3568(2002)052[0019:LRSFES]2.0.CO;2

Li, W., Cao, S., Campos-Vargas, C., Sanchez-Azofeifa, A., 2017. Identifying tropical dry forests extent and succession via the use of machine learning techniques. Int. J. Appl. Earth Obs. Geoinf. 63, 196–205. https://doi.org/10.1016/j.jag.2017.08.003

Lovell, J.L., Jupp, D.L.B., Culvenor, D.S., Coops, N.C., 2003. Using airborne and ground-based ranging lidar to measure canopy structure in Australian forests. Can. J. Remote Sens. 29, 607–622. https://doi.org/10.5589/m03-026

Mallet, C., Bretar, F., 2009. ISPRS Journal of Photogrammetry and Remote Sensing Full-waveform topographic lidar : State-of-the-art. ISPRS J. Photogramm. Remote Sens. 64, 1–16. https://doi.org/10.1016/j.isprsjprs.2008.09.007

Marquette, C.M., 2006. Settler welfare on tropical forest frontiers in Latin America. Popul. Environ. 27, 397–444. https://doi.org/10.1007/s11111-006-0029-y

Martínez-Garza, C., González-Montagut, R., 1999. Seed rain from forest fragments into tropical pastures in Los Tuxtlas, Mexico. Plant Ecol. 145, 255–265. https://doi.org/10.1023/A:1009879505765

Meeussen, C., Govaert, S., Vanneste, T., Calders, K., Bollmann, K., Brunet, J., Cousins, S.A.O., Diekmann, M., Graae, B.J., Hedwall, P.O., Krishna Moorthy, S.M., Iacopetti, G., Lenoir, J., Lindmo, S., Orczewska, A., Ponette, Q., Plue, J., Selvi, F., Spicher, F., Tolosano, M., Verbeeck, H., Verheyen, K., Vangansbeke, P., De Frenne, P., 2020. Structural variation of forest edges across Europe. For. Ecol. Manage. 462, 117929. https://doi.org/10.1016/j.foreco.2020.117929

Muss, J.D., Aguilar-amuchastegui, N., Mladenoff, D.J., Henebry, G.M., 2013. Analysis of Waveform Lidar Data Using Shape-Based Metrics. IEEE Geosci. Remote Sens. Lett. 10, 106–110. https://doi.org/https://doi.org/10.1109/LGRS.2012.2194472

Novotný, J., Navrátilová, B., Janoutová, R., Oulehle, F., Homolová, L., 2020. Influence of site-specific conditions on estimation of forest above ground biomass from airborne laser scanning. Forests 11, 1–18. https://doi.org/10.3390/f11030268

Olson, D.M., Dinerstein, E., Wikramanayake, E.D., Burgess, N.D., Powell, G.V.N., Underwood, E.C., Amico, J.A.D., Itoua, I., Strand, H.E., Morrison, J.C., Loucks, J., Allnutt, T.F., Ricketts, T.H., Kura, Y., Lamoreux, J.F., Wesley, W., Hedao, P., Kassem, K.R., 2001. Terrestrial Ecoregions of the World : A New Map of Life on Earth 51, 933–938.

Portillo-Quintero, C.A., Sánchez-Azofeifa, G.A., 2010. Extent and conservation of tropical dry forests in the Americas. Biol. Conserv. 143, 144–155. https://doi.org/10.1016/j.biocon.2009.09.020

Quesada, M., Sanchez-Azofeifa, G.A., Alvarez-Añorve, M., Stoner, K.E., Avila-Cabadilla, L., Calvo-Alvarado, J., Castillo, A., Espírito-Santo, M.M., Fagundes, M., Fernandes, G.W., Gamon, J., Lopezaraiza-Mikel, M., Lawrence, D., Morellato, L.P.C., Powers, J.S., Neves, F. de S., Rosas-Guerrero, V., Sayago, R., Sanchez-Montoya, G., 2009. Succession and management of tropical dry forests in the Americas: Review and new perspectives. For. Ecol. Manage. 258, 1014–1024. https://doi.org/10.1016/j.foreco.2009.06.023

Ruiz, L.A., Hermosilla, T., Mauro, F., Godino, M., 2014. Analysis of the Influence of Plot Size and LiDAR Density on Forest Structure Attribute Estimates. Forests 936–951. https://doi.org/10.3390/f5050936

Sánchez-Azofeifa, G.A., Guzmán-Quesada, J.A., Vega-Araya, M., Campos-Vargas, C., Durán, S.M., D'Souza, N., Gianoli, T., Portillo-Quintero, C., Sharp, I., 2017. Can terrestrial laser scanners (TLSs) and hemispherical photographs predict tropical dry forest succession with liana abundance? Biogeosciences 14, 977–988. https://doi.org/10.5194/bg-14-977-2017

Sánchez-Azofeifa, G.A., Quesada, M., Rodríguez, J.P., Jafet, M., Stoner, K.E., Castillo, A., Garvin, T., Zent, Egleé L, Calvo-, J.C., Kalacska, M.E.R., Fajardo, L., Gamon, J.A., Cuevas-, P., Sanchez-azofeifa, G.A., Quesada, M., Rodriguez, J.P., Nassar, J.M., Stoner, K.E., Castillo, A., Garvin, T., Zent, Eglee L, Calvo-alvarado, J.C., Kalacska, M.E.R., Fajardo, L., Gamon, J.A., Forestal, D.I., Manejo, P. De, Recursos, C. De, Rica, I.T.D.C., 2005. Research Priorities for Neotropical Dry Forests Published by : Association for Tropical Biology and Conservation Stable URL : https://www.jstor.org/stable/30043216 Research Priorities for Neotropical Dry Forests '. Biotropica.

Schnitzer, S.A., Heijden, G. Van Der, Mascaro, J., Walter, P., Schnitzer, S.A., Heijden, G. Van Der, Mascaro, J., Carson, W.P., 2014. Lianas in gaps reduce carbon accumulation in a tropical forest Published by : Wiley on behalf of the Ecological Society of America Stable URL : http://www.jstor.org/stable/43495216 Lianas in

gaps reduce carbon accumulation in a tropical forest. Ecology 95, 3008–3017. https://doi.org/https://doi.org/10.1890/13-1718.1

Skowronski, N.S., Clark, K.L., Gallagher, M., Birdsey, R.A., Hom, J.L., 2014. Airborne laser scanner-assisted estimation of aboveground biomass change in a temperate oak-pine forest. Remote Sens. Environ. 151, 166–174. https://doi.org/10.1016/j.rse.2013.12.015

Zhao, G., Sanchez-azofeifa, A., Laakso, K., Sun, C., Fei, L., 2021. Hyperspectral and Full-Waveform LiDAR Improve Mapping of Tropical Dry Forest ' s Successional Stages. Remote Sens. https://doi.org/https://doi.org/10.3390/rs13193830

Zhao, K., Popescu, S., Nelson, R., 2009. Lidar remote sensing of forest biomass: A scale-invariant estimation approach using airborne lasers. Remote Sens. Environ. 113, 182–196. https://doi.org/10.1016/j.rse.2008.09.009

2. Chapter 2: Characterizing Transitions between Successional Stages in a Tropical Dry Forest using LiDAR Techniques

2.1 Introduction

Tropical dry forest (TDF) ecosystems are dominated by deciduous species (trees and lianas), have total annual precipitation ranges from 700 to 2000mm, and the mean annual temperature is ≥ 25 °C (Sánchez-Azofeifa et al., 2005). TDFs contain a wealth of biodiversity and essential habitats for wildlife (Kalacska et al., 2007), and in combination with other tropical ecosystems, play a significant role in climate regulation and the carbon cycle (Novotný et al., 2020). Furthermore, TDFs are a critical source of ecosystem services (Calvo-Rodriguez et al., 2016; Cao et al., 2015). However, up to the beginning of the 21st century, nearly 98% of all TDFs suffered destruction worldwide, and the rate of disturbance and deforestation far surpasses land use and land cover change processes in other tropical biomes (Hoekstra et al., 2005). Moreover, it was estimated that only 40% of all tropical dry forests in the Americas were left in 2010, although these remnants were highly fragmented (Portillo-Quintero and Sánchez-Azofeifa, 2010).

Despite the high rate of tropical dry forest deforestation, some areas in the Americas, due to changes in socio-economic conditions, are reverting the deforestation process, and the landscape is now a mosaic of tropical secondary forests (Cao et al., 2015). This landscape, classification denoted as “agro-landscapes”, is defined a**s** sites where forests emerge between agricultural systems and where regeneration depends upon a combination of factors, including land-use history, germination of seeds transported via biotic and abiotic vectors, as well as recovery of

remnant vegetation (Burrough, 2001; Janzen, 1986; Martínez-Garza and González-Montagut, 1999).

Tropical dry forest succession is a natural and complex ecological process affected by climatic and land use history processes (Quesada et al., 2009; Sánchez-Azofeifa et al., 2017). Associated to these processes, diverging opinions exist on the characterization of TDF based on the successional stage or age since abandonment (Quesada et al., 2009). Most work associated with the characterization of tropical dry forests succession has been led by Kalacska et al. (2004, 2005, 2007) and Arroyo-Mora et al. (2005). Kalacska et al. (2004, 2005, 2007) provided important baselines for structural properties and their association with the Holdridge Complexity Index, which in turn were used for TDF characterization using hyperspectral remote sensing data (Kalacska et al., 2005). Arroyo-Mora et al. (2005) proposed a well-accepted definition of successional stages in TDFs: based on (1) the horizontal and vertical structure, (2) leaf flushing dynamics, and (3) the density of green canopy cover. This definition characterizes TDF along a continuum divided into three principal successional stages, i.e., early, intermediate, and late. Near the boundary of these successional stages, the species composition of leaf-litter invertebrates changes, small mammal populations develop alterations in their behavioral and biological characteristics, and the number and structure of bird communities alter (Laurance et al., 2002; Manu et al., 2007; Portillo-quintero et al., 2013). Under the approaches proposed by Kalácska et al. (2005) and Arroyo-Mora et al. (2005), different successional stages derive noticeable differences in horizontal and vertical forest structures such as canopy height, canopy gaps, leaf area index (LAI), and photosynthetically active radiation (PAR). These differences have been extended to generate TDF classifications by Castillo et al. (2011, 2012), Gu et al. (2018), and more

recently Zhao et al. (2021), which combined advanced machine learning classifiers to generate advanced forest cover maps based on age and succession.

Remote sensing technologies, either active (such as LiDAR and SAR) or passive (optical), have been proven to have the potential to quantify secondary TDFs succession (Castillo-Núñez et al., 2011; Kalacska et al., 2007). In particular, LiDAR provides a new way to characterize forest structure (Bagaram et al., 2018; Bouvier et al., 2015; Clark et al., 2004). LiDAR systems have the capacity to penetrate dense forest canopies, making it easier to detect the vertical distribution of forest structural components than with optical spectroscopy (Drake et al., 2002). LiDAR applications in forestry can be categorized into airborne laser scanning (ALS) and terrestrial laser scanner (TLS) according to different systems platforms. Among ALS sensors, discrete ALS (ALS_D) is traditionally used to estimate stand attributes or classify tree species (Bottalico et al., 2017) and forest canopy fuel (Ruiz et al., 2014). However, little attention has been attributed to full-waveform ALS (ALS_{FW}) because of the raw waveform data's complexity and lack of processing software (Crespo-peremarch et al., 2018). ALS_{FW} sensors can avoid the drawbacks of ALS_D by sampling as a continuous return signal to provide information within vertical forest components beyond the first and last returns. Furthermore, information from ALS_{FW} sensors has been effectively correlated to changes in the vertical distribution of sub-canopy components of boreal forests as well as the neotropical rainforest (Crespo-Peremarch et al., 2020; Leafsky et al., 2002).

Over the years, ALS_{FW} has been applied widely to study vegetation and forest inventories using various methods; Chaulagain et al. (2022) studied modelling hydraulic roughness in the presence of riparian vegetation using field-based and LiDAR-based data. Crespo-Peremarch et al. (2020) investigated the independent

capability of ALS_{FW}, ALS_{D} and TLS to estimate the spatial distribution of understory vegetation from the lower strata (height < 4m) for two structurally contrasting conifer dominated forests. The result of this work indicated that understory vegetation density classes can be determined more accurately with ALS_{FW} than ALS_{D} or TLS. The first approach (ALS_{FW}) by Castillo et al. (2011, 2012) demonstrated that changes in the vertical forest structure (such as height), are associated with the main successional stages (early, intermediate, and late) of a secondary TDF could be effectively identified using ALS_{FW} data. In their results, the spatial agreement between the ISODATA classification and the "literature-based" classification was 97%, 56%, and 99% for the early, intermediate, and late successional stages, respectively. Furthermore, Muss et al. (2013) were the first to propose the use of centroids and the radius of gyration (RG) of the ALS_{FW} to predict forest biomass in northern Wisconsin. Gu et al. (2018) identified successional stages of a TDF in Costa Rica using ALS_{FW} and demonstrated that shape-based metrics (such as centroids and the radius of gyration) can be used to detect those ecological successional stages. Working in the same study area, Zhao et al. (2021) assessed the ability of hyperspectral images and LiDAR data to map ecological succession with respect to a given age attribute and not the discrete age groups or successional stages. These studies give evidence that approaches based on ALS_{FW} can be successfully implemented to characterize changes in TDF's structure.

The common denominator of the former studies is that their products are basically deterministic. Deterministic classification approaches consider that the presence between forest boundaries of different successional stages/ages is not continuous, ignoring the fact that transitions are present between these boundaries. Until today, with the exception of Li et al. (2017) and Zhao et al. (2021), most work in the mapping and characterization of TDFs has ignored the subtle differences present

among the principal successional stages as they deterministically divide secondary forests into early, intermediate, and late successions as mentioned above (Figure 1). In this context, this paper aims to be the first one to assess how well ALS_{FW} characterizes the structural properties of transition between different TDF successional stages. Here we seek the answer to the following questions: (1) How does the canopy height change along the successional path? (2) How do structural parameters derived from full-waveform Airborne LiDAR and its associated metrics change across transition linking intermediate to late forest succession? This work expands on previous studies by Li et al. (2017) and Sánchez-Azofeifa et al. (2017), who proposed mapping secondary TDFs succession should consider transition between principal successional stages but did not identify their characterization. So, our work will try to fill this gap.

2.2 Materials and Methods

2.2.1 Study Area

The study was conducted in an area of approximately 50 km^2 at the Santa Rosa National Park Environmental Monitoring Super Site (SRNP-EMSS), located in the northwest of the Guanacaste province in Costa Rica (10°48′53″ N, 85°36′54″ W) (Figure 2). The topography of the study area is relatively flat, although there are some hills and even small cliffs in the eastern parts. SRNP-EMSS is located at a TDF with a mean annual temperature of 25 °C and annual precipitation of 1720 mm. Most precipitation occurs in the wet season from June to November, and water availability is extremely limited in the 6-month dry season lasting from December to May (Sánchez-Azofeifa et al., 2005). SRNP-EMSS is a mosaic of diverse vegetation communities with pastures and secondary forests in different gradients of succession (Zhao et al., 2021). Before the national park was established in 1971, SRNP-EMSS had

suffered intense deforestation since the early 1600s, resulting from natural and anthropogenic disturbances such as forest fires, agriculture and timber extraction (Kalacska et al., 2004). Drought deciduous species dominate the vegetation. The area has forest patches in three successional stages: early, intermediate and late. Of these, 80-100%, 30-50% and 10-40% of woody plants are deciduous during the dry season in early, intermediate and late-stage forests, correspondingly (Arroyo-Mora et al., 2005).

2.2.2 Data Acquisition

2.2.2.1 Forest cover map

This study uses a forest cover map with a combination of age and succession compiled by Zhao et al. (2021) to identify the transition zones of the study area, which is the only goal of using this data set in this study. Zhao et al. (2021) created the map by combining hyperspectral (HyMap) and waveform LiDAR data LVIS (Land Vegetation and Ice Sensor) acquired in 2005 over the study area (Fig. 2b). The map has a 1m-by-1m spatial resolution and five age groups: 0—10, 10—20, 20—30, 30—50 and 50+ years. The map was compiled using age-attribute metrics that were used as entry-level variables on a randomized nonlinear archetypal analysis (RNAA) model to select the most informative metrics to map different successional stages (Zhao et al., 2021). After that, they adopted a relative attribute learning (RAL) algorithm for independent and fused metrics to learn the relative attribute levels of the forest ages. In the map, the age attributes of a TDF are considered a continuous expression of relative attribute scores/levels that change along the process of ecological succession. Furthermore, the fusion of four HyMap metrics and five LVIS metrics significantly

improves the accuracy of the generated forest age map. Additional information can be found in Zhao et al. (2021).

2.2.2.2 Full-waveform LiDAR

Once the known transition regions were identified using the forest cover map, we used a colorized small footprint (1m*1m) full-waveform airborne LiDAR data set with two main goals: (1) to create a canopy height model (CHM) to quantify canopy height changes along the cross-section between intermediate and late forests, as well as their transition; and (2) to characterize vertical structure differences of plots in transitions and main successional stages based on the corresponding leaf area density profile and several shape-based metrics. The full-waveform LiDAR data set was acquired on May 21, 2021 by Stereocarto (Madrid, Spain) using a RIEGL LMS-Q680i sensor (Riegl Laser Measurement Systems GmbH, Horn, Austria). The aircraft used for this work is a Piper Azteca PA23. For the execution of the flight, the LiteMapper IGI 6800i System (sn. 10-0104) that integrates into the same platform a LiDAR system RIEGL LMS-Q680i, a Photogrammetric camera DigiCAM H5D-50, Video Camera, and GPS INS, equipped with an electronic device for the compensation of the drag of the image and microprocessor for the automatic control of the exposure. Relevant flight parameters are shown in Table 1.

2.2.3 Data Processing

2.2.3.1 Transition identification

Transition connecting early (0—10 years), intermediate (10—30 years) and late (30—50+ years) forest patches were used in this study. All patches with an area less or equal to 5000 m^2 were selected and removed from the forest cover map by Zhao et al.

(2021). This was done to standardize the transitions between forest patches. Once the select and remove operation was performed, a 25m buffer was created around all three principal successional stages, extracting the overlap between each of them as their respective transitions (Portillo-quintero et al., 2013).

2.2.3.2 Estimation of canopy height variation

The ALS_{FW} data was used to create a high-resolution canopy height model image (1m*1m) after it was denoised, classified, interpolated and normalized (Figure 3). The "cloth" simulation filter (CSF) algorithm was used to classify ground points and off-ground points (Zhang et al., 2016), which were interpolated into a DEM (from ground points) and DSM (from off-ground points) using Delaunay triangulations (Isenburg et al., 2006a, 2006b). Especially for huge data sets processing, such as our full-waveform Airborne LiDAR data in this study, Delaunay triangulations is faster, more robust and pro vides better results than other methods, including inverse distance weighting (IDW), natural neighbors, Kriging, and splines, etc. (Isenburg et al., 2006b, 2006a). After that, the DSM was used to subtract the DEM to derive the canopy height model (CHM). For the overlapped part of two datasets (Figure 2d), a local maximum filter (LMF) with a fixed 3*3 windows size was applied to the smoothed CHM (1m*1m) to find the local highest or local maxima within its peaks. These local maxima points correspond to individual tree-top locations and heights, so we can segment individual trees and extract corresponding canopy height information for three main successional stages and two transitions. One limitation of this method is it will underestimate the result because CHM is a raster image that understories cannot be detected. A univariate analysis of variance (ANOVA) for canopy height and the successional stage was conducted to study the effect of the successional stages on vertical structure (canopy height).

2.2.3.3 Canopy height comparison between transitions and main successional stages

Here, we made efforts to identify the change in canopy height between transitions and other main successional stages. More specifically, emphasis was placed on the intermediate, transition II, and late successional stages. In this context, it refers to the successional stage from intermediate to late when the "transition II" is mentioned. The canopy height model was interpolated from 1m*1m to 5m*5m using bilinear interpolation (Smith, 1981) to make the canopy heights change smoother and more realistic. We then randomly and evenly selected twenty cross-sections of 500m length along four different successional paths (Intermediate — Transition II— Intermediate, Intermediate — Transition II— Late, Late —Transition II— Intermediate— Transition II— Late, Intermediate — Transition II— Late — Transition II— Intermediate) in the study area (Figure 3) to extract canopy height values so as to generate vertical profiles. Also, forest canopy gaps were avoided as much as possible when selecting these twenty cross-sections over the study area (Bagaram et al., 2018).

2.2.3.4 Estimation of vertical forest structure

Besides canopy height information derived from CHM, full-waveform LiDAR data provides valuable understory information. In this section, twenty-seven of the 45m*45m plots were selected randomly along nine cross-sections (Intermediate – Transition II– Late) to capture the inter-stage (Transition II) and intra-stage (Intermediate and Late) forest structure for further analysis (Figure 3) using Airborne LiDAR data, including the estimation of Leaf Area Index (LAI), and the generation of a Leaf Area Density profile. LAI represents the area of leaves per unit of ground area ($m^2 \cdot m^{-2}$) (de Almeida et al., 2019). In this study, LAI was calculated for each plot

using a gap fraction approach that is based on the Beer-Lambert Law. Beer-Lambert Law describes quantitively the attenuation process of light penetrating into the canopy:

$$e^{-k*LAI_z} = \frac{I_z}{I_0} \quad (1)$$

Where k is the extinction coefficient, LAI is the effective leaf area index, I_z is PAR transmittance at canopy depth z, and I_0 is the total incoming Photosynthetically Active Radiation (PAR). The value of k is affected by the view zenith angle and the leaf angle distribution. Assuming that the leaves' individual size is small enough compared to the canopy and leaves are randomly distributed (Kalacska et al., 2007), the gap fraction can be equivalent to transmittance (Bréda, 2003). The expression for k should be:

$$k = k(\theta, \alpha) = \frac{G(\theta, \alpha)}{\cos(\theta)} \quad (2)$$

Where θ is the view zenith angle, α is the leaf angle distribution, and $G(\theta, \alpha)$ is the G-function, which corresponds to the fraction of foliage projected onto the plane normal to the zenith direction (Bouvier et al., 2015). The leaf angle describes the spatial distribution information of the foliage, and the spherical model can simply and reliably simulate the distribution of leaf angles. Thus, we assumed the foliage distributes randomly, and leaf angles distribute as a spherical distribution (Vose et al., 1995). Through Beer-Lambert Law, LAI and gap fraction ($P(\theta)$) could be connected:

$$P(\theta) = e^{-G(\theta,\alpha)*LAI/\cos(\theta)} \quad (3)$$

For direct-lighting conditions, the gap fraction was estimated by the ratio between the number of returns below a specified height threshold and the total number of returns (Bouvier et al., 2015). Cumulative LAI at a given canopy depth z can therefore be calculated through the fraction of Photosynthetically Active Radiation (PAR) that is

transmitted at canopy depth z using the following adaptation of the Beer–Lambert Law:

$$LAI_z = -\frac{ln(P_z)}{k} \quad (4)$$

Where LAI_z is the leaf area index value for layer z; P_z is the gap fraction from the top of the canopy to a given height z. We calculated LAI using a k-value of 0.5 for all twenty-seven plots in this study (Martens et al., 1993). It is logical that different k-values might affect the derived LAI value; however, it would not significantly change the profile shapes. Besides, all LAI profiles were calculated from gap fractions at each height interval with the given thickness d_z as 0.5m in this study. The resulting LAI_z values were then divided by d_z to derive the vertical profile of canopy height versus Leaf Area Density, LAD. The LAD distribution is expressed as the leaf area at each height interval per canopy volume ($m^2 \cdot m^{-3}$). Therefore, LAD values are the partial volumetric components of LAI (Almeida et al., 2019).

2.2.3.5 Derivation of LiDAR metrics

Gu et al. (2018) analyzed the potential of 21 LiDAR metrics from LVIS (Land Vegetation and Ice Sensor) system to differentiate and quantify TDF successions and proved that some of these metrics were significantly different between successional stages (Table 3). Using the shape of the Leaf Area Density profile, we calculated seven metrics for each plot along the cross-section: x coordinate of the centroid (C_x), y coordinate of the centroid (C_y), the radius of gyration (RG), the x coordinate of the maximum waveform amplitude (P_x); and the y coordinate of the maximum waveform amplitude (P_y); the maximum tree height (H_{max}); the Leaf Area Index (LAI) (Figure 4).

We also conducted the univariate analysis of variance (ANOVA) to describe the effect of the successional stages on LiDAR metrics and forest structure parameters.

We paid particular attention to shape-based metrics, including centroid components (C) and the radius of gyration (RG), to understand how the vertical profile changes along the transition. C represents the centroid and is also called the center for mass in physics, which could be visualized as "the balance point" of the waveform (Muss et al., 2013). It is feasible to detect the waveform's shape, and distribution relative to the ground in the LAD profile through C. RG is the root mean square of the sum of distances for all points, which would fluctuate with the relative area of each peak in the waveform's modality. RG allows an understanding of how the waveform is distributed around its centroid. This permits the use of the waveform's shape better than just the centroid itself. RG can be visualized as the relationship between the total length of the vertical profile and its shape and position (Muss et al., 2013), which could be expressed as:

$$RG = \sqrt{\frac{\sum(x_i - C_x)^2 + \sum(y_i - C_y)^2}{n}} \quad (5)$$

These three shape-based metrics were mainly used in LiDAR waveforms to describe the motion of objects and the manner in which material is distributed around an axis (Muss et al., 2013). Apart from these, we also proposed to derive P_x and P_y (x and y coordinates of the maximum waveform amplitude, respectively) to capture waveform distribution features.

2.3 Results

2.3.1 Transitions

Figure 5 shows that intermediate and late successions (denoted in blue and rose, respectively) account for a large percentage of forest patches at the SRNP-EMSS, whereas only small areas of early succession are present (yellow parts) (Figure 3 & Figure 5). As a result, transition II (from intermediate to late successions) dominates the entire study area. Thus, apart from small areas representing transition I (from early to intermediate successions), most transitions belong to type II. On the other hand, because of abundant species diversity, more considerable variability in canopy openness and significant differences in species composition are shown in intermediate and late successional stages (Calvo-Rodriguez et al., 2021). So, the subsequent study will focus specifically on transition II.

2.3.2 Changes in canopy height across transitions

An overall view of the canopy height range distribution of the CHM over the three successional stages and two transitions (Figure 6) show a straightforward continuous process with the canopy heights increasing along the succession based on individual tree segmentation. More specifically, the average canopy height in the early successional stage is nearly 6m, while that of the intermediate and the late successional stages are 12m and 16m, respectively. The canopy height range of transition I and transition II is mainly distributed between 7m to 12m and 13m to 16m, respectively. The late successional stage and transition II show higher values of standard deviation for canopy height in comparison with the early succession and transition I stages (Table 3). The ANOVA results (Table 3) indicate that canopy height and successional

gradients are statistically different, and those differences are significant ($F_{(4,80495)}$=8329.7; $p<0.05$).

More detailed, within some random areas (instead of all forest patches for each entire stage), Figure 7 shows the change in canopy height along the path of succession from twenty cross-section profiles with a 500 meter length, containing four different order combinations over the study area. From the violin plot (Figure 6) and twenty cross-section profiles, we captured a general trend in canopy height along the path of succession: the canopy height increases with the successional stages (Intermediate — Transition II— Late). However, if we capture the canopy height changes through some specific transects, different findings can be shown: a constant change in the canopy height of the three successional stages can be seen in Figure 7 (g), Figure 7 (j), and Figure 7 (t). In detail, Figure 7 (g) shows the value in transition II is even higher than that of the late; however, the canopy height of the late stage is obviously higher than that of the intermediate stage. On the other hand, some solid ups and downs in light blue highlight parts (transition II) suggest that the instability and significant transition features in the successional stage from the intermediate to the late (Figure 7 (c), (e), (f), (m), (n) and (o)), which is unique compared with other primary successional stages.

2.3.3 Forest structure characteristics of transitions

The LAD versus canopy height profiles were extracted for the twenty-seven plots along nine cross-sections that have two different successional stages and one transition (i.e., Intermediate stage, Transition II and Late stage). Figure 8 shows the profile waveform variation in plots. The results show, that in general, the plots in the intermediate successional stage are characterized by two peaks feature: one peak is at the above-ground height of approximately 11m (Figure 8. (a)), and the other occurs at

the elevation of 0.5-1.0m. Besides, a slight stratified phenomenon is shown. In contrast, highly stratified plots from the late stage derived a LAD profile with constantly changed LAD values and multiple peaks occurring at 0-5m, 10-15m and 18-22m (Figure 8. (c)). On the other hand, similar to the intermediate stage, some plots in the transition II also show two peaks feature similar to that of the intermediate stage. The elevation of the first peak increases slightly to 10-15m (Figure 8. (b)), and the other is still at 0.5-1m; however, other plots show a moderate but not strongly stratified trend, which shows the waveform distribution is becoming more irregular compared with the intermediate stage.

Using the LAD profiles, five LiDAR metrics (C_x, C_y, RG, P_x and P_y) and two forest structure parameters (H_{max} and LAI) were derived (Table 4 and Figure 9). Three shape-based LiDAR metrics (C_x, C_y and RG) significantly differentiated between successional stages ($p<0.05$). At the same time, P_x and P_y do not show significant differences for various successional stages ($p1=0.09>0.05$, $p2=0.72>0.05$). Moreover, the intermediate successional plots showed higher values of leaf area density (0.31) than transition II (0.28) and late plots (0.25). In contrast, the values of C_y and H_{max} increase with the three successional stages: from 8.69 to 10.30 (intermediate stage to transition II) to 13.00 (transition II to late stage) and from 17.47 to 20.36 (intermediate stage to transition II) to 25.75 (transition II to late stage), respectively. However, a fluctuation in C_y and H_{max} of transition II and the late stage was shown through the higher standard deviation value compared to the intermediate successional stage. Similarly, plots associated with transition II and the late successional stage yielded an RG value with a more significant standard deviation (Table 4). The results also suggest that there is an increase in the leaf area index (LAI) with the successional gradient. This is most likely because of the growth of vegetation and a higher abundance of mixed

species along the successional gradient from early to late: the highest LAI values are associated with the late successional stage (LAI=12.61), the lowest with the intermediate successional stage (LAI=10.79), and moderate to the transition II (LAI=11.47).

2.4 Discussion

Previous traditional approaches used to detect the succession of secondary TDFs have followed deterministic strategies that define sharp boundaries between different successional stages. More recent studies by Li et al. (Li et al., 2017) linked canopy height range to successional stages (i.e., 0 m to 7m, 7.1 m to 13.7 m and 13.71 m to 35 m for early, intermediate, and late successional stages, respectively). Their strategy was to define forest successional stages based on empirical canopy height ranges extracted from LVIS data (Castillo et al., 2012) and field data (Kalacska et al., 2004). Nevertheless, the authors stopped sort of trying to find the relationship between the canopy heights and two transitions. Uncertainties between transitions existing and different successional stages were ignored. In this study, we considered the regrowth process of secondary TDFs as a continuous stochastic phenomenon (Li et al., 2017). We first identified three successional stages at the SRNP-EMSS based on the forest age and then defined the buffer areas of these stages as transition zones. These are important, because differences in species composition, photosynthetic active radiation (PAR), and forest structure manifest themselves in transitions, which also affect the soil moisture conditions and micro-climate (Kalacska et al., 2004, 2007). According to our results, after decades of regrowth, few forest patches currently exist in the early stage or transition I stage at the SRNP-EMSS up to 2021 (Figure 3, Table 3). As expected, the median canopy height shows a positive trend from 6.1 m in the early

stage to 12.68m in the intermediate stage to 16.3 m in the late stage (Table 3). This result can be validated by study area's inventory data by Kalacska et al. (2007). The intermediate, transition II and the late stage have higher standard deviations of canopy heights because of complex multi-layers of vegetation, such as mature trees, deciduous species of woody plants (with the existence of lianas), shrubs etc.

Within a forest patch, all vegetation, including canopy, understory, and shrubs, compete for sunlight and water or nutrition from the soil, which leads to variable tree heights within the same stage. The other factor might be the presence of lianas, especially in intermediate, transition II and late successional stages. Although lianas account for a small percentage (less than 10%) of the above-ground biomass in tropical forests, they represent a large proportion (up to 40%) of leaf productivity (Han and Sánchez-azofeifa, 2022; Ingwell et al., 2010; Rodríguez-Ronderos et al., 2016; Schnitzer, 2005). Some forest structures, such as canopy height and plant area, can essentially decrease with liana infestation (Sánchez-Azofeifa et al., 2017); because lianas and host trees also compete for available above- and under-ground resources, which include incoming solar radiation (above-ground) and nutrition (under-ground**)** in forest stands (Paul and Yavitt, 2011). For instance, a liana-infested plot had more irregular canopies with heights from 10m to 20m, whereas the surrounding forest patches had significantly taller canopies from 25m to 35m (Figure 7c). Even in Figure 7j,k,r,t, there is no apparent changes in canopy height with successions. This may be explained as the lianas infestation.

According to Li et al. (2017) and Sánchez-Azofeifa et al. (2017), we carefully selected 27 plots including 9 intermediate, 9 transition and 9 late successional stage sites along the successional path. Forest structure characteristics for mid-canopy and understory were identified from full-waveform LiDAR data and metrics derived from

the LAD profile waveform. In particular, the waveform information is sensitive to changes in structural attributes along the path of succession due to the vertical distribution of biomass in varying successional stages (Castillo et al., 2012). The intermediate successional stage with monotonous vegetation structures is characterized by shorter trees and relatively sparser shrubs than transition II and late successional stages, which leads to two distinct peaks on the vertical profile (Figure 8a). One is caused by the single strata of sparse canopy crowns at an elevation of 8 - 12m, while the other is at 0.5 - 2m due to pastures or shrubs. Within forest regeneration plots, mixed species, including higher canopy, abundant understory, and even dense shrubs, dominate the forest patches in the late successional stage, leading to more vertical layers (Figure 8c). Nonetheless, in the case of the transition II, the waveform distribution shows moderate changes when compared to the characteristics from the intermediate and late successional stages. In some plots, the apparent "two peaks" feature could still be seen because of the existence of a dense canopy and sparse understory, similar to that of the intermediate stage. There was a noticeable increase in the elevation of the upper canopy peak in transition II when compared to the intermediate stage, though. Besides, more plots in transition II show a relatively smooth waveform change (i.e., noticeable but not strongly stratified) caused by a higher abundance of vertical layers and biomass. A recent study (Cao et al., 2016) demonstrated that the intermediate stage has a higher growth rate than the late successional stage, which could be interpreted as a change in the species composition and vegetation density in transition I and II.

Regarding the comparison of metrics derived from the vertical profile, several forest structure parameters such as C_y, H_{max}, LAI, and biomass had statistically significant differences along the successional gradients (Table 4 and Figure 9b); in

contrast, there are no such differences in P_x and P_y with successional gradients (Table 4 and Figure 9c, d). The reasonable explanation to this is that almost all forest patches in the intermediate, transition II and late successional stages at the SRNP-EMSS are covered by dense shrubs, tall grasses, or short trees, leading to the corresponding maximum peak in the vertical profile of all three successional stages. The value of P_x is affected by LAI as a function of understory components (pastures, shrubs, and lianas) along the successional trajectory of a TDF, so that the increasing trend could be seen from intermediate, transition II to late successional stages. The standard deviations of these metrics reflect variations in the waveform distribution along the different successional stages (Table 4). C_x is moving to left in the LAD profile along the successional path (Intermediate – Transition II - Late); this can be explained as most lianas put on leaves leading to overestimating LAD. Furthermore, the intermediate stage is infested by lianas most seriously, and lianas abundance decreases from the intermediate to the late stage. This is because canopy gaps decrease from the intermediate to the late stage, leading to the lack of sunlight. As a result, more lianas are killed in transition II and the late stage. So, the value of LAD decreases with succession. Besides, as mentioned above, the variation of canopy height within one successional stage due to lianas tangles will cause a higher standard deviation for C_y, especially for transition II and the late successional stages. In addition, the transition II and the late stages create more heterogeneous space compared to the intermediate stage, which is captured by the variability in RG (Figure 10). The higher value of RG, reflected as an irregular waveform distribution in vertical profiles, may be interpreted as resulting from heterogeneity in the forest, unevenly aged trees, and mixed species. A clear distinction between the intermediate and late successional stages can be seen in Figure 10 which links the RG metric to the LAD metric. However, plots in the transition II show a prominent transition feature, which spreads among the

intermediate and late stages. We also can see a few green triangles are much away from others (Figure 10), which might be caused by misclassification from the forest cover map. There were statistically significant changes in shape-based metrics (centroid and RG), and thus these metrics can significantly differentiate successional stages. This highlights the importance of taking advantage of the overall vertical structures of forests in identifying the succession of TDFs. It also highlights how the process of ecological succession is a combination of transitional forest types along a stochastic path instead of one that is deterministic.

It is worth mentioning that the smoothing involved in the derivation of raster products may have influenced the ability to distinguish between successional stages. Smoothing effects may mute emergent species signals , which are often present in late-stage successional forests. Further, in tropical forests and especially tropical dry forests, one must consider the effects of lianas on the forest structure (Schnitzer et al., 2014). In some cases, trees infested by liana tangles probably never evolve into the following successional gradient, although they are getting older. This, however, is beyond the original scope of the study. One potential issue identified in this study is that the forest cover map (Zhao et al., 2021) is based on LVIS data acquired in 2005; whereas the Stereocarto full-waveform LiDAR was acquired in 2021. Forests are dynamic and likely to change dramatically over 16 years, but they were changing together. In other words, the sequence of succession did not change. In the case of our study, the 2005 data (the forest cover map) was simply used to locate regions of interest (transitions). Once the known transition regions were identified the 2021 data (Stereocarto full-waveform LiDAR data) was used to confirm their unique structure. In doing so, we have successfully shown that transitions have and maintain their unique structural identity as transitions between the established successional stages.

2.5 Conclusions

This study characterized the inter-successional stages (transitions) of a tropical dry forest at the Santa Rosa National Park, Guanacaste, Costa Rica, using full-waveform airborne LiDAR data. Our work highlights: (1) the potential of the LiDAR technique in studying the succession of TDFs; (2) that the process of ecological succession is a combination of transitional forest types along a stochastic path instead of deterministic in nature as discussed before; (3) that forest structures of transitions show interesting variations in vertically and horizontally with that of principal successional stages along the successional gradient; and (4) that shape-based metrics can successfully capture the variability of the different waveform distribution, which is expected to change with the vertical structure. We proposed unique characteristics and the ecological significance of transitions, specifically transition II (from intermediate to late successional stages). Although my study is limited to one single site in Costa Rica this is the first step to exploring and understanding forest structural characteristics of inter-successional stages or transitions in TDFs.

2.6 References

Arroyo-Mora, J.P., Sánchez-Azofeifa, G.A., Kalacska, M., Rivard, B., Calvo-Alvarado, J.C., Janzen, D.H., 2005. Secondary Forest Detection in a Neotropical Dry Forest Landscape Using Landsat 7 ETM + and IKONOS Imagery Published by : Association for Tropical Biology and Conservation Stable URL : https://www.jstor.org/stable/30043218 REFERENCES Linked references are. Biotropica 37, 497–507.

Bagaram, M.B., Giuliarelli, D., Chirici, G., Giannetti, F., Barbati, A., 2018. UAV remote sensing for biodiversity monitoring: Are forest canopy gaps good covariates? Remote Sens. 10, 1–28. https://doi.org/10.3390/rs10091397

Bottalico, F., Chirici, G., Giannini, R., Mele, S., Mura, M., Puxeddu, M., Mcroberts, R.E., Valbuena, R., Travaglini, D., 2017. International Journal of Applied Earth Observation and Geoinformation Modeling Mediterranean forest structure using airborne laser scanning data. Int. J. Appl. Earth Obs. Geoinf. 57, 145–153. https://doi.org/10.1016/j.jag.2016.12.013

Bouvier, M., Durrieu, S., Fournier, R.A., Renaud, J., 2015. Remote Sensing of Environment Generalizing predictive models of forest inventory attributes using an area-based approach with airborne LiDAR data. Remote Sens. Environ. 156, 322–334. https://doi.org/10.1016/j.rse.2014.10.004

Bréda, N.J.J., 2003. Ground-based measurements of leaf area index: A review of methods, instruments and current controversies. J. Exp. Bot. 54, 2403–2417. https://doi.org/10.1093/jxb/erg263

Burrough, P.A., 2001. GIS and geostatistics: Essential partners for spatial analysis. Environ. Ecol. Stat. 8, 361–377. https://doi.org/10.1023/A:1012734519752

Calvo-Rodriguez, S., Sanchez-Azofeifa, A.G., Duran, S.M., Espírito-Santo, M.M., 2016. Assessing ecosystem services in Neotropical dry forests: A systematic review. Environ. Conserv. https://doi.org/10.1017/S0376892916000400

Calvo-Rodriguez, S., Sánchez-Azofeifa, G.A., Durán, S.M., Espírito-Santo, M.M. Do, Nunes, Y.R.F., 2021. Dynamics of carbon accumulation in tropical dry forests

under climate change extremes. Forests 12, 1–15. https://doi.org/10.3390/f12010106

Cao, S., Sanchez-Azofeifa, G.A., Duran, S.M., Calvo-Rodriguez, S., 2016. Estimation of aboveground net primary productivity in secondary tropical dry forests using the Carnegie-Ames-Stanford approach (CASA) model. Environ. Res. Lett. 11. https://doi.org/10.1088/1748-9326/11/7/075004

Cao, S., Yu, Q., Sanchez-Azofeifa, A., Feng, J., Rivard, B., Gu, Z., 2015. Mapping tropical dry forest succession using multiple criteria spectral mixture analysis. ISPRS J. Photogramm. Remote Sens. 109, 17–29. https://doi.org/10.1016/j.isprsjprs.2015.08.009

Castillo-Núñez, M., Sánchez-Azofeifa, G.A., Croitoru, A., Rivard, B., Calvo-Alvarado, J., Dubayah, R.O., 2011. Delineation of secondary succession mechanisms for tropical dry forests using LiDAR. Remote Sens. Environ. 115, 2217–2231. https://doi.org/10.1016/j.rse.2011.04.020

Castillo, M., Rivard, B., Sánchez-Azofeifa, A., Calvo-Alvarado, J., Dubayah, R., 2012. LIDAR remote sensing for secondary Tropical Dry Forest identification. Remote Sens. Environ. 121, 132–143. https://doi.org/10.1016/j.rse.2012.01.012

Chaulagain, S., Stone, M.C., Dombroski, D., Gillihan, T., Chen, L., Zhang, S., 2022. An investigation into remote sensing techniques and field observations to model hydraulic roughness from riparian vegetation. River Res. Appl. 1730–1745. https://doi.org/10.1002/rra.4053

Clark, M.L., Clark, D.B., Roberts, D.A., 2004. Small-footprint lidar estimation of sub-canopy elevation and tree height in a tropical rain forest landscape. Remote Sens. Environ. 91, 68–89. https://doi.org/10.1016/j.rse.2004.02.008

Crespo-peremarch, P., Ángel, L., Balaguer-beser, Á., Estornell, J., Cartography, G., Sensing, R., Cgat, G., València, U.P. De, Vera, C. De, 2018. ISPRS Journal of Photogrammetry and Remote Sensing Analyzing the role of pulse density and voxelization parameters on full- waveform LiDAR-derived metrics. ISPRS J. Photogramm. Remote Sens. 146, 453–464. https://doi.org/10.1016/j.isprsjprs.2018.10.012

Crespo-Peremarch, P., Fournier, R.A., Nguyen, V.T., van Lier, O.R., Ruiz, L.Á., 2020. A comparative assessment of the vertical distribution of forest components using full-waveform airborne, discrete airborne and discrete terrestrial laser scanning data. For. Ecol. Manage. 473, 118268. https://doi.org/10.1016/j.foreco.2020.118268

de Almeida, D.R.A., Stark, S.C., Shao, G., Schietti, J., Nelson, B.W., Silva, C.A., Gorgens, E.B., Valbuena, R., Papa, D. de A., Brancalion, P.H.S., 2019. Optimizing the remote detection of tropical rainforest structure with airborne lidar: Leaf area profile sensitivity to pulse density and spatial sampling. Remote Sens. 11. https://doi.org/10.3390/rs11010092

Drake, J.B., Dubayah, R.O., Clark, D.B., Knox, R.G., Blair, J.B., Hofton, M.A., Chazdon, R.L., Weishampel, J.F., Prince, S.D., 2002. Estimation of tropical forest structural characteristics using large-footprint lidar. Remote Sens. Environ. 79, 305–319. https://doi.org/https://doi.org/10.1016/S0034-4257(01)00281-4

Gu, Z., Cao, S., Sanchez-Azofeifa, G.A., 2018. Using LiDAR waveform metrics to describe and identify successional stages of tropical dry forests. Int. J. Appl. Earth Obs. Geoinf. 73, 482–492. https://doi.org/10.1016/j.jag.2018.07.010

Han, T., Sánchez-azofeifa, G.A., 2022. Extraction of Liana Stems Using Geometric Features from Terrestrial Laser Scanning Point Clouds. Remote Sens. https://doi.org/https://doi.org/10.3390/rs14164039

Hoekstra, J.M., Boucher, T.M., Ricketts, T.H., Roberts, C., 2005. Confronting a biome crisis: Global disparities of habitat loss and protection. Ecol. Lett. 8, 23–29. https://doi.org/10.1111/j.1461-0248.2004.00686.x

Ingwell, L.L., Joseph Wright, S., Becklund, K.K., Hubbell, S.P., Schnitzer, S.A., 2010. The impact of lianas on 10 years of tree growth and mortality on Barro Colorado Island, Panama. J. Ecol. 98, 879–887. https://doi.org/10.1111/j.1365-2745.2010.01676.x

Isenburg, M., Liu, Y., Shewchuk, J., Snoeyink, J., 2006a. Streaming computation of delaunay triangulations. ACM Trans. Graph. 25, 1049–1056. https://doi.org/10.1145/1141911.1141992

Isenburg, M., Liu, Y., Shewchuk, J., Snoeyink, J., Thirion, T., 2006b. Generating raster DEM from mass points via TIN streaming. Lect. Notes Comput. Sci. (including Subser. Lect. Notes Artif. Intell. Lect. Notes Bioinformatics) 4197 LNCS, 186–198. https://doi.org/10.1007/11863939_13

Janzen, D.H., 1986. The Future of Tropical Ecology Author (s): Daniel H . Janzen Source : Annual Review of Ecology and Systematics , Vol . 17 (1986), pp . 305-324 Published by : Annual Reviews Stable URL : http://www.jstor.org/stable/2096998 THE FUTURE OF TROPICAL ECOLOG. For. Ecol. Manage. 17, 305–324.

Kalácska, M., Calvo-Alvarado, J.C., Sánchez-Azofeifa, G.A., 2005. Calibration and assessment of seasonal changes in leaf area index of a tropical dry forest in different stages of succession. Tree Physiol. 25, 733–744. https://doi.org/10.1093/treephys/25.6.733

Kalacska, M., Member, S., Sanchez-azofeifa, G.A., Caelli, T., Rivard, B., Boerlage, B., 2005. Using Bayesian Networks. IEEE Trans. Geosci. Remote Sens. 43, 1866–1873. https://doi.org/https://doi.org/10.1109/TGRS.2005.848412

Kalacska, M., Sanchez-Azofeifa, G.A., Calvo-Alvarado, J.C., Quesada, M., Rivard, B., Janzen, D.H., 2004. Species composition, similarity and diversity in three successional stages of a seasonally dry tropical forest. For. Ecol. Manage. 200, 227–247. https://doi.org/10.1016/j.foreco.2004.07.001

Kalacska, M., Sanchez-azofeifa, G.A., Rivard, B., Caelli, T., 2007. Ecological fingerprinting of ecosystem succession : Estimating secondary tropical dry forest structure and diversity using imaging spectroscopy. Remote Sens. Environ. 108, 82–96. https://doi.org/10.1016/j.rse.2006.11.007

Laurance, W.F., Lovejoy, T.E., Vasconcelos, H.L., Bruna, E.M., Didham, R.K., Stouffer, P.C., Gascon, C., Bierregaard, R.O., Laurance, S.G., Sampaio, E., 2002. Ecosystem Decay of Amazonian Forest Fragments : a 22-Year Investigation. Ecosyst. Decay Amaz. Fragm. 16, 605–618.

Leafsky, M.A.., Cohen, W.B.., Parker, G.G.., Harding, D.J., 2002. Lidar Remote Sensing for Ecosystem Studies. Bioscience 52, 19–30. https://doi.org/https://doi.org/10.1641/0006-3568(2002)052[0019:LRSFES]2.0.CO;2

Li, W., Cao, S., Campos-Vargas, C., Sanchez-Azofeifa, A., 2017. Identifying tropical dry forests extent and succession via the use of machine learning techniques. Int. J. Appl. Earth Obs. Geoinf. 63, 196–205. https://doi.org/10.1016/j.jag.2017.08.003

Manu, S., Peach, W., Cresswell, W., 2007. The effects of edge , fragment size and degree of isolation on avian species richness in highly fragmented forest in West Africa 287–297.

Martens, S.N., Ustin, S.L., Rousseau, R.A., 1993. Estimation of tree canopy leaf area index by gap fraction analysis. For. Ecol. Manage. 61, 91–108. https://doi.org/10.1016/0378-1127(93)90192-P

Martínez-Garza, C., González-Montagut, R., 1999. Seed rain from forest fragments into tropical pastures in Los Tuxtlas, Mexico. Plant Ecol. 145, 255–265. https://doi.org/10.1023/A:1009879505765

Muss, J.D., Aguilar-amuchastegui, N., Mladenoff, D.J., Henebry, G.M., 2013. Analysis of Waveform Lidar Data Using Shape-Based Metrics. IEEE Geosci. Remote Sens. Lett. 10, 106–110. https://doi.org/https://doi.org/10.1109/LGRS.2012.2194472

Novotný, J., Navrátilová, B., Janoutová, R., Oulehle, F., Homolová, L., 2020. Influence of site-specific conditions on estimation of forest above ground biomass from airborne laser scanning. Forests 11, 1–18. https://doi.org/10.3390/f11030268

Paul, G.S., Yavitt, J.B., 2011. Tropical Vine Growth and the Effects on Forest Succession: A Review of the Ecology and Management of Tropical Climbing Plants. Bot. Rev. 77, 11–30. https://doi.org/10.1007/s12229-010-9059-3

Portillo-quintero, C., Sánchez-azofeifa, A., Espírito-santo, M.M., 2013. Edge Influence on Canopy Openness and Understory Microclimate in Two Neotropical Dry Forest Fragments 157–172.

Portillo-Quintero, C.A., Sánchez-Azofeifa, G.A., 2010. Extent and conservation of tropical dry forests in the Americas. Biol. Conserv. 143, 144–155. https://doi.org/10.1016/j.biocon.2009.09.020

Quesada, M., Sanchez-Azofeifa, G.A., Alvarez-Añorve, M., Stoner, K.E., Avila-Cabadilla, L., Calvo-Alvarado, J., Castillo, A., Espírito-Santo, M.M., Fagundes, M., Fernandes, G.W., Gamon, J., Lopezaraiza-Mikel, M., Lawrence, D., Morellato, L.P.C., Powers, J.S., Neves, F. de S., Rosas-Guerrero, V., Sayago, R., Sanchez-

Montoya, G., 2009. Succession and management of tropical dry forests in the Americas: Review and new perspectives. For. Ecol. Manage. 258, 1014–1024. https://doi.org/10.1016/j.foreco.2009.06.023

Rodríguez-Ronderos, M.E., Bohrer, G., Sanchez-Azofeifa, A., Powers, J.S., Schnitzer, S.A., 2016. Contribution of lianas to plant area index and canopy structure in a Panamanian forest. Ecology 97, 3271–3277. https://doi.org/10.1002/ecy.1597

Ruiz, L.A., Hermosilla, T., Mauro, F., Godino, M., 2014. Analysis of the Influence of Plot Size and LiDAR Density on Forest Structure Attribute Estimates. Forests 936–951. https://doi.org/10.3390/f5050936

Sánchez-Azofeifa, G.A., Guzmán-Quesada, J.A., Vega-Araya, M., Campos-Vargas, C., Durán, S.M., D'Souza, N., Gianoli, T., Portillo-Quintero, C., Sharp, I., 2017. Can terrestrial laser scanners (TLSs) and hemispherical photographs predict tropical dry forest succession with liana abundance? Biogeosciences 14, 977–988. https://doi.org/10.5194/bg-14-977-2017

Sánchez-Azofeifa, G.A., Quesada, M., Rodríguez, J.P., Jafet, M., Stoner, K.E., Castillo, A., Garvin, T., Zent, Egleé L, Calvo-, J.C., Kalacska, M.E.R., Fajardo, L., Gamon, J.A., Cuevas-, P., Sanchez-azofeifa, G.A., Quesada, M., Rodriguez, J.P., Nassar, J.M., Stoner, K.E., Castillo, A., Garvin, T., Zent, Eglee L, Calvo-alvarado, J.C., Kalacska, M.E.R., Fajardo, L., Gamon, J.A., Forestal, D.I., Manejo, P. De, Recursos, C. De, Rica, I.T.D.C., 2005. Research Priorities for Neotropical Dry Forests Published by : Association for Tropical Biology and Conservation Stable URL : https://www.jstor.org/stable/30043216 Research Priorities for Neotropical Dry Forests '. Biotropica.

Schnitzer, S.A., 2005. A mechanistic explanation for global patterns of liana abundance and distribution. Am. Nat. 166, 262–276. https://doi.org/10.1086/431250

Schnitzer, S.A., Heijden, G. Van Der, Mascaro, J., Walter, P., Schnitzer, S.A., Heijden, G. Van Der, Mascaro, J., Carson, W.P., 2014. Lianas in gaps reduce carbon accumulation in a tropical forest Published by : Wiley on behalf of the Ecological Society of America Stable URL : http://www.jstor.org/stable/43495216 Lianas in gaps reduce carbon accumulation in a tropical forest. Ecology 95, 3008–3017. https://doi.org/https://doi.org/10.1890/13-1718.1

Smith, P.R., 1981. Bilinear interpolation of digital images. Ultramicroscopy 6, 201–204. https://doi.org/10.1016/S0304-3991(81)80199-4

Vose, J.M., Sullivan, N.H., Clinton, B.D., Bolstad, P. V., 1995. Vertical leaf area distribution, light transmittance, and application of the Beer-Lambert Law in four mature hardwood stands in the southern Appalachians. Can. J. For. Res. 25, 1036–1043. https://doi.org/10.1139/x95-113

Zhang, W., Qi, J., Wan, P., Wang, H., Xie, D., Wang, X., Yan, G., 2016. An easy-to-use airborne LiDAR data filtering method based on cloth simulation. Remote Sens. 8, 1–22. https://doi.org/10.3390/rs8060501

Zhao, G., Sanchez-azofeifa, A., Laakso, K., Sun, C., Fei, L., 2021. Hyperspectral and Full-Waveform LiDAR Improve Mapping of Tropical Dry Forest' s Successional Stages. Remote Sens. https://doi.org/https://doi.org/10.3390/rs13193830

2.7 Tables

Table 1. Technical specifications of the flight parameters and sensors of the study. Data were acquired in the SRNP-EMSS on May 21, 2021. Abbreviations: GSD=ground sampling distance, FOV=field of view.

	Parameters	Data
Piper PA-23-250 Azteca D aircraft	Average flight height over the field (H)	500 m
	Flight speed	158 km/h
	Scanning frequency	266,000 points/s
DigiCAM H5D-50	Field Pixel Size (GSD)	6.0 cm
	Width of stripes	488 m
	FOV	60°
	Longitudinal overlaps	60%
	Transverse overlaps	50%
RIEGL LMS-Q680i	Average density	36 points/m^2

Table 2. LiDAR metrics are used to characterize a waveform as a function of the successional stage (after Gu et al. (2018)).

Type	Metrics	Description
Point-based	P_x	x coordinate of the maximum waveform amplitude
	EC	The total bin number of the effective waveform
	RH50	Height at which 50% of the waveform energy occurs
Area-based	AH1e10	Total waveform amplitude where the relative height is less than 10m
	AH1015	Total waveform amplitude where the relative height is between 10m and 15m
	AH1520	Total waveform amplitude where the relative height is between 15m and 20m
Shape-based	C_x	The x coordinate of the waveform centroid
	C_y	The y coordinate of the waveform centroid
	RG	The radius of gyration

Table 3. Mean values with one standard deviation of canopy height with three successional stages and two transitions at the SRNP-EMSS were extracted from LiDAR data. Significant differences (F values) according to the successional stages are presented from ANOVA. Height was extracted in meters and tree individuals per stage.

Successional stages	Mean height (m)	Tree individuals per stage
Early	6.07±1.91	1545
Ecotone I: Early to Intermediate	9.42±2.84	3546
Intermediate	12.68±2.98	22470
Ecotone II: Intermediate to Late	14.09±3.17	23815
Late	16.28±3.70	29124
ANOVA	8329.7*	N/A

* p value < 0.05.

Table 4. Mean (±SD) of metrics derived from the full-waveform LiDAR along the nine cross-sections over two successional stages and one transition in the dry forest at the SRNP-EMSS, Guanacaste, Costa Rica. Significant differences (F values) according to different successional stages are provided. C_x, the x coordinate of the waveform centroid; C_y, the y coordinate of the waveform centroid; RG, the radius of gyration; P_x, the x coordinate of the maximum waveform amplitude; P_y, the y coordinate of the maximum waveform amplitude; H_{max}, maximum tree height (m); LAI, leaf area index.

Metrics	Intermediate	Ecotone II	Late	ANOVA
C_x	0.31 ± 0.03	0.28 ± 0.03	0.25 ± 0.04	6.87*
C_y	8.69 ± 0.87	10.30 ± 1.75	13.00 ± 1.78	17.64*
RG	5.13 ± 0.43	5.96 ± 1.01	7.52 ± 1.02	17.55*
P_x	0.73 ± 0.14	0.75 ± 0.22	0.78 ± 0.15	0.09
P_y	2.31 ± 3.38	1.25 ± 0.43	1.41 ± 0.79	0.72
H_{max}	17.47 ±1.50	20.36 ± 3.49	25.75 ± 3.54	17.61*
LAI	10.79 ± 1.34	11.47 ± 1.23	12.61 ± 0.83	5.71*

*p-value < 0.05

2.8 Figures

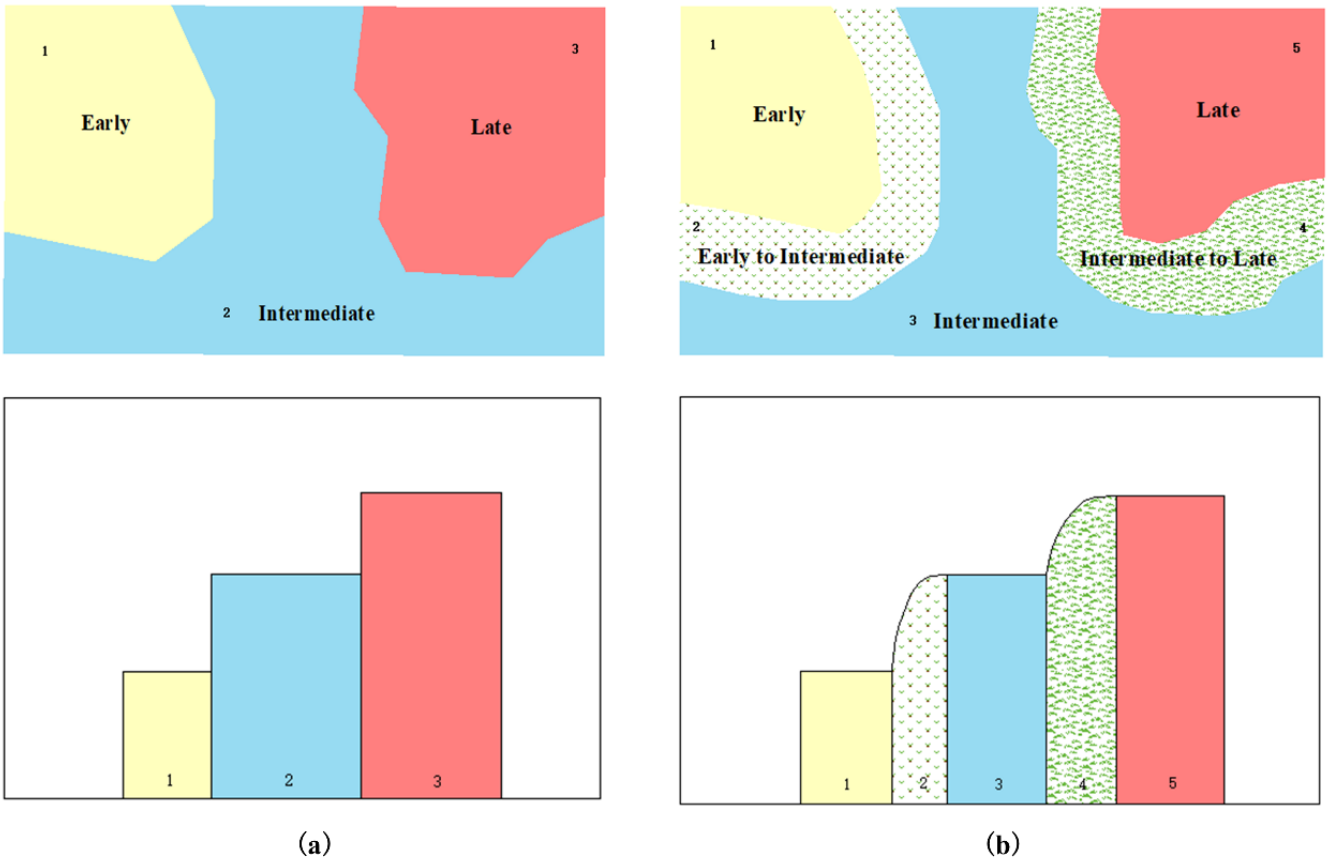

Figure 1. The traditional and refined principles for mapping secondary TDFs succession. (a) Traditional definitions assume that different successional stages (1, 2 and 3) have deterministic extents. (b) Approaches considering the presence of transitions (such as 2 and 4) between the principal successional stages 1, 3 and 5.

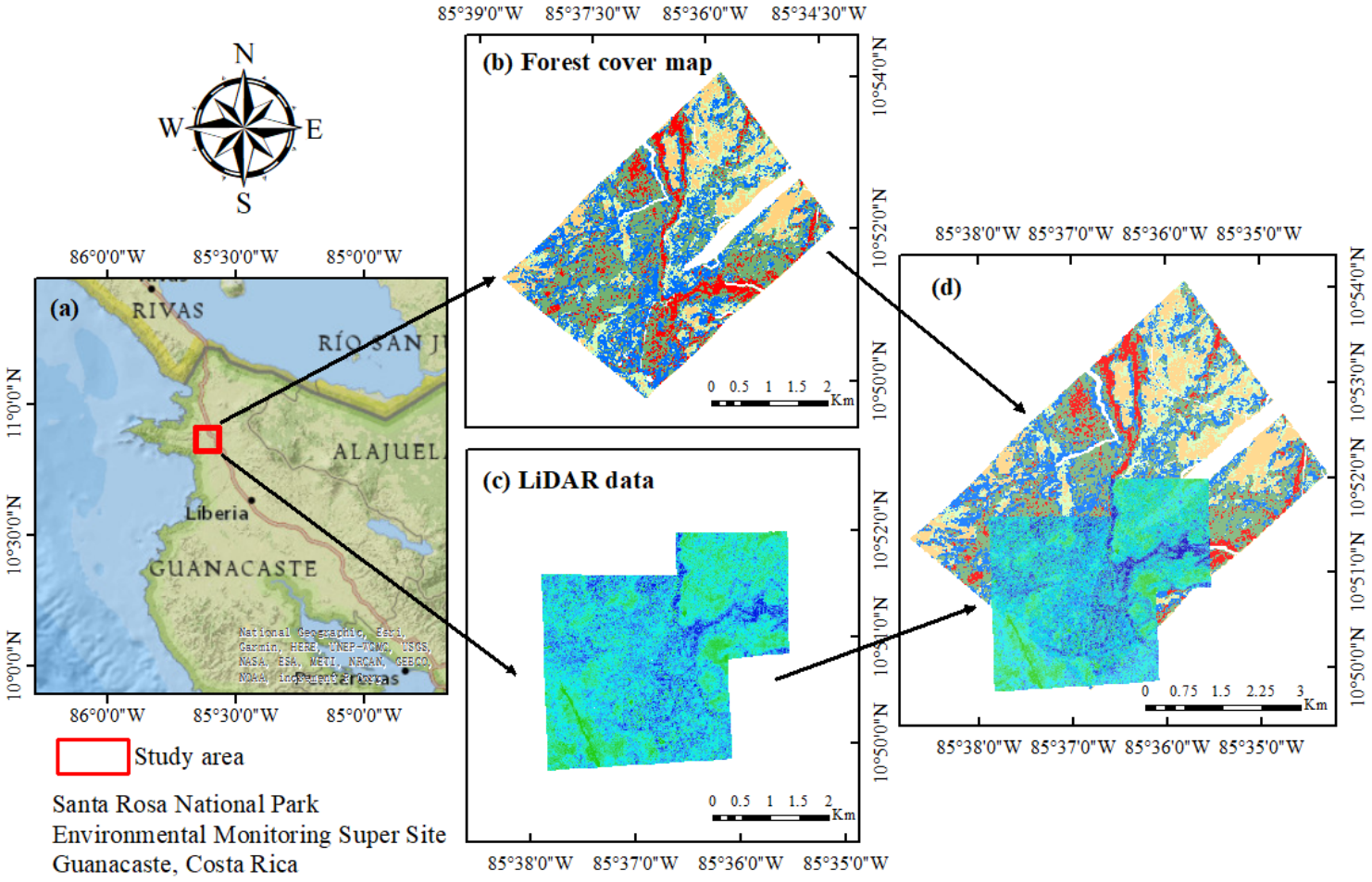

Figure 2. The study area at the Santa Rosa National Park Environmental Monitoring Super Site (SRNP-EMSS), Guanacaste, Costa Rica (a), the forest cover map from Zhao et al. (2021) generated with LVIS and HyMap data in (b), Riegl Full-waveform Airborne LiDAR data 2021, acquired in SRNP-EMSS (c), the datasets from subfigures (b,c) overlay each other to define the study area.

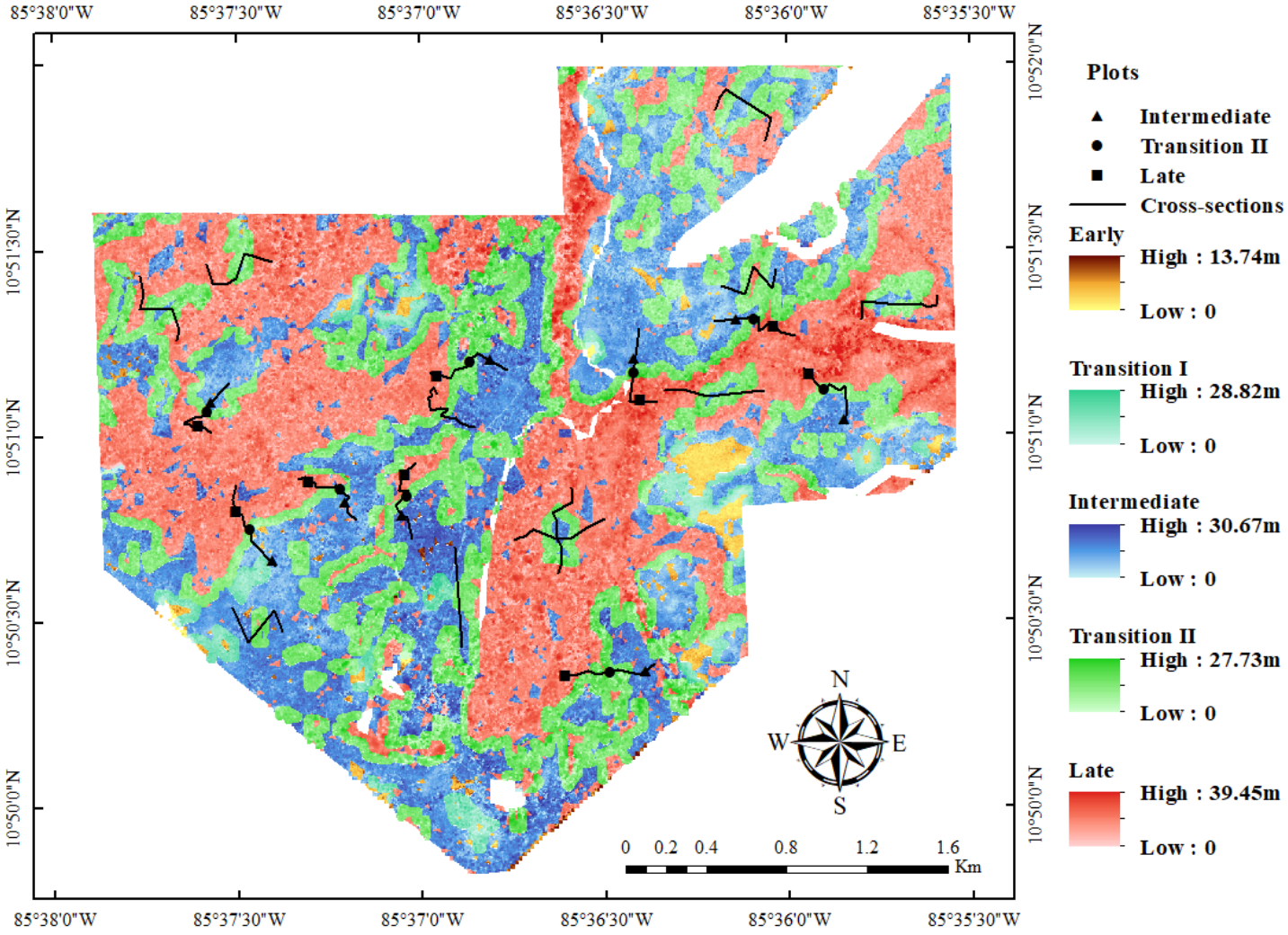

Figure 3. A canopy height model with a 5 m × 5 m spatial resolution derived from Airborne LiDAR data and the spatial distribution of three successional stages and two transitions at the SRNP-EMSS, Guanacaste, Costa Rica. The range is the overlapping between the forest cover map (Zhao et al., 2021) and full-waveform LiDAR data (Figure 2d). Twenty cross-sections (black lines) of 500 m in length and twenty-seven plots (nine for each successional stage) with an area of 45m*45m along the successional gradient were extracted randomly and evenly over the study area.

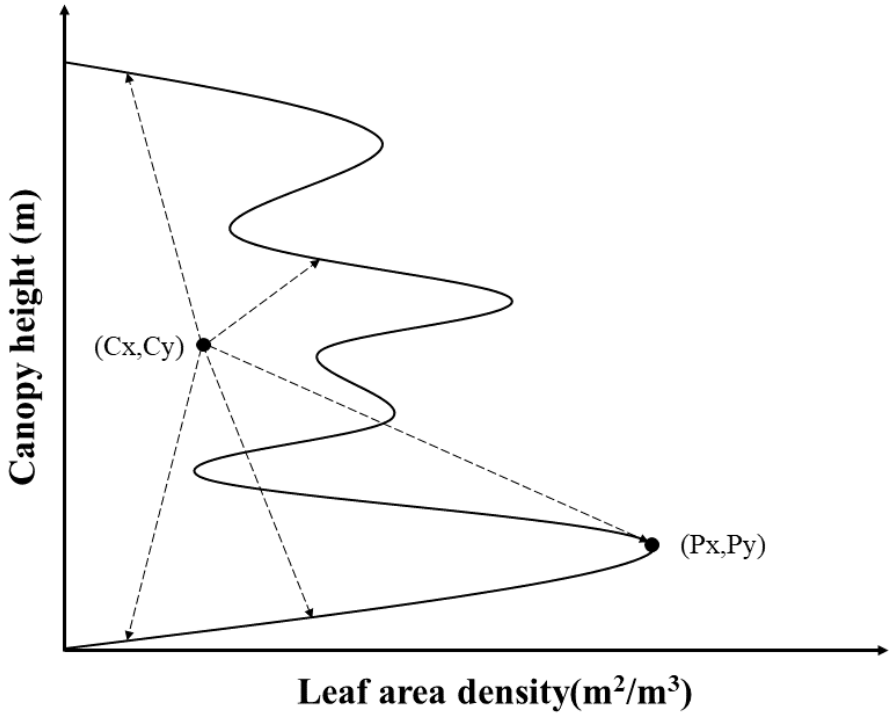

Figure 4. The figure describes the centroid (C_x and C_y), the radius of gyration (RG), and the coordinate of maximum waveform amplitude (P_x and P_y) based on the LAD profile waveform (after Muss et al. (2013)).

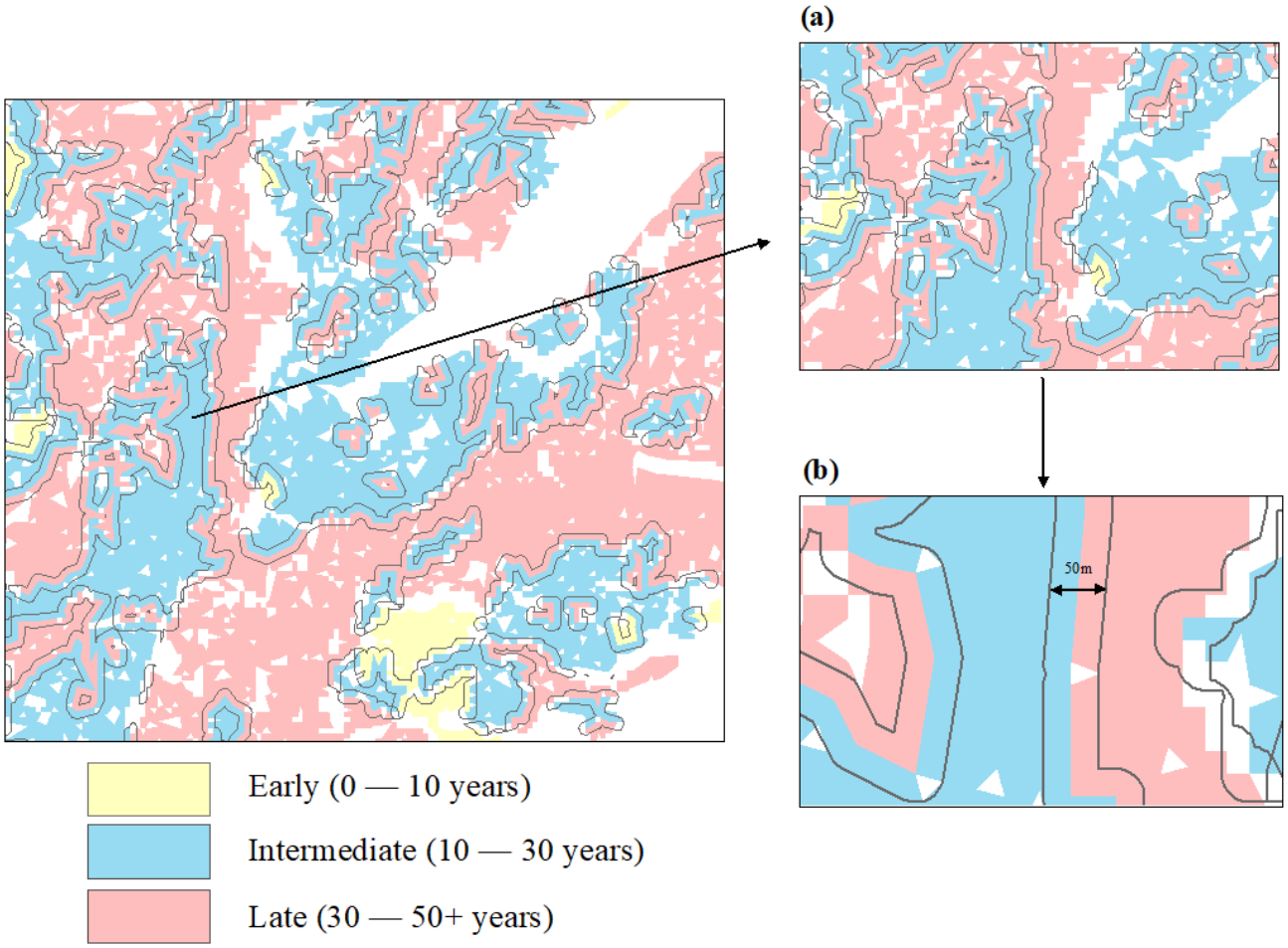

Figure 5. Transitions were extracted by building a 25m buffer from the forest age map, which was defined into three principal successional stages according to age (Zhao et al., 2021). To improve the accuracy and reasonability of transition zone extraction, some forest patches with small areas (< 5000 m^2 in early, < 10,000 m^2 in intermediate, and < 2000 m^2 in late) were dropped (i.e., white dots represent data gaps and strips represent invalid noise). (a,b) are examples and magnifications a selected transition zone at the SRNP-EMSS, Guanacaste, Costa Rica.

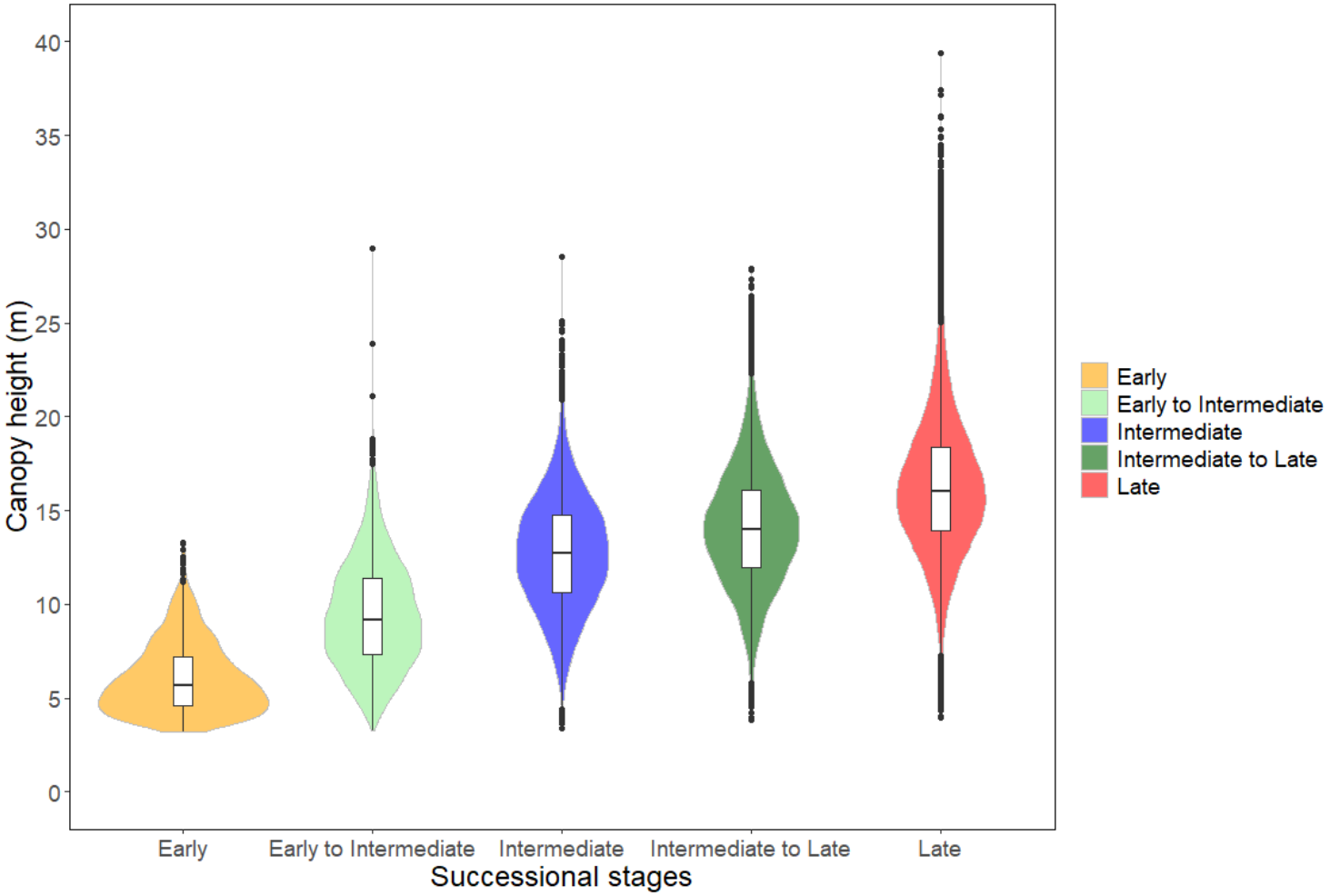

Figure 6. Canopy height variability of successional stages at the SRNP-EMSS, Guanacaste, Costa Rica, derived from a canopy height model (CHM) over Early, Transition I: Early to Intermediate, Intermediate, Transition II: Intermediate to Late, and Late successional stages.

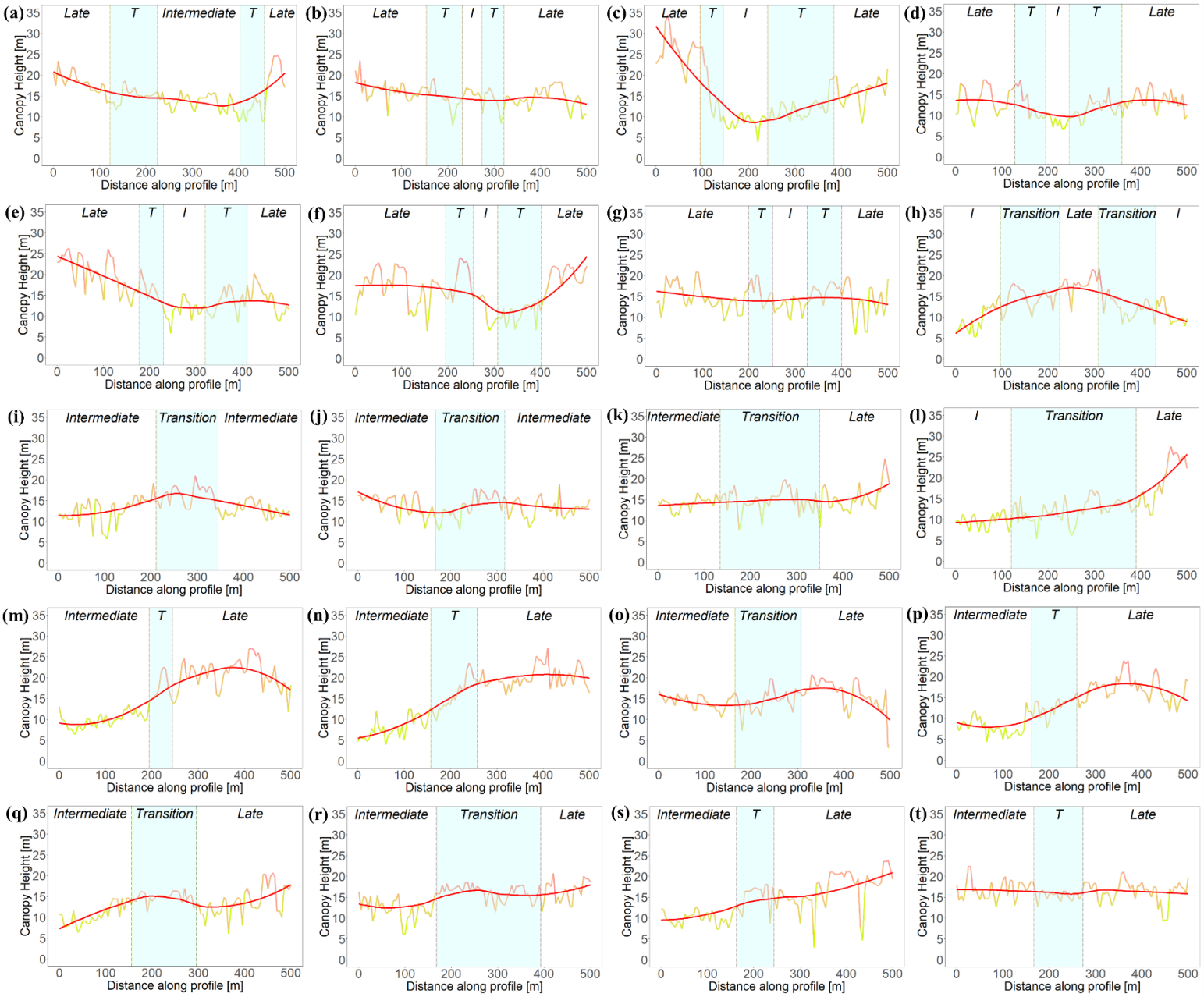

Figure 7. Twenty profiles were derived from randomly selected cross-sections along the path of succession at the SRNP-EMSS (Figure 3). The x-axis is the distance along the profile (i.e., 0 — 500m). The y-axis is canopy height in meters (the range: 0 — 35m). "I" refers to the intermediate successional stage and "T" refers to transition II (from Intermediate to Late successional stage). (a–g) describe the change in canopy height along the Late–Transition II–Intermediate–Transition II–Late; (h) describes the change in canopy height along the Intermediate–Transition II–Late–Transition II–Intermediate; (i,j) describe the change in canopy height along the Intermediate–Transition II–Intermediate; (k–t) describe the change in canopy height along the Intermediate–Transition II–Late (all transitions refer to the successional stage from intermediate to late). Transition II is highlighted in light blue. The solid red line represents a fitted smooth change trend.

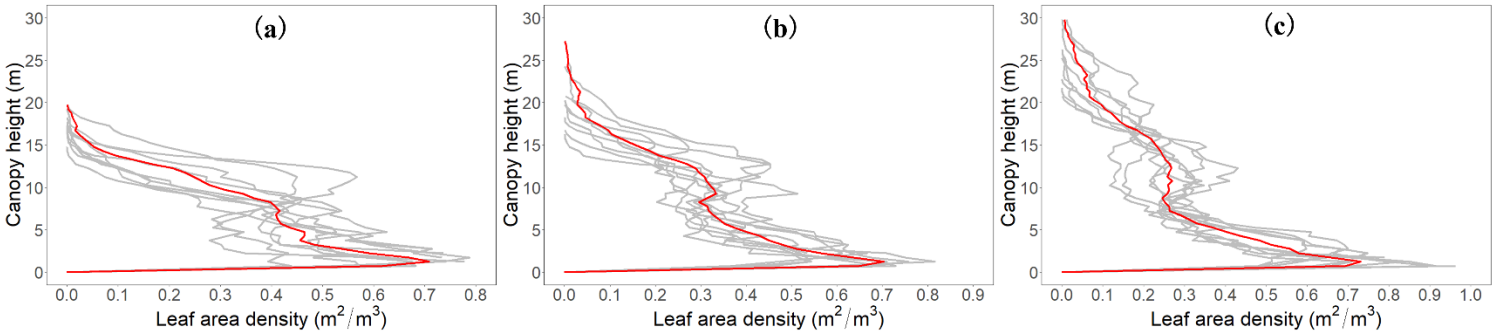

Figure 8. The vertical LAD profile of the nine plots for the Intermediate (a), Transition II (b), and Late successional stage (c). The solid red line in each subfigure is the average for the corresponding nine waveforms.

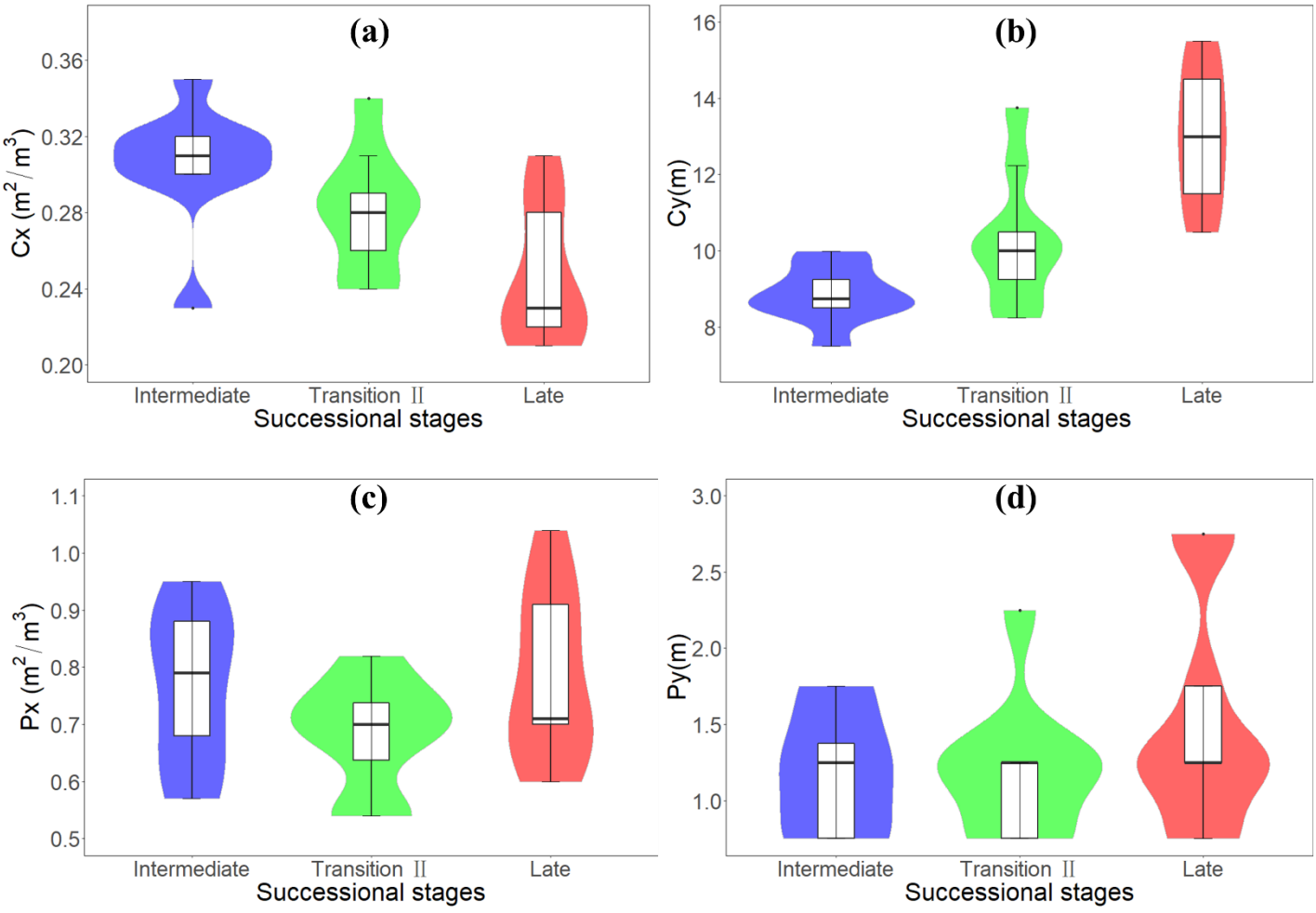

Figure 9. Violin plots for the LiDAR metrics (C_x, C_y, P_x and P_y) distribution along the forest successional gradients (Intermediate — Transition II— Late) from 27 plots at the SRNP-EMSS, Guanacaste, Costa Rica. C_x, the x coordinate of the waveform centroid; C_y, the y coordinate of the waveform centroid; P_x, the x coordinate of the maximum waveform amplitude; P_y, the y coordinate of the maximum waveform amplitude.

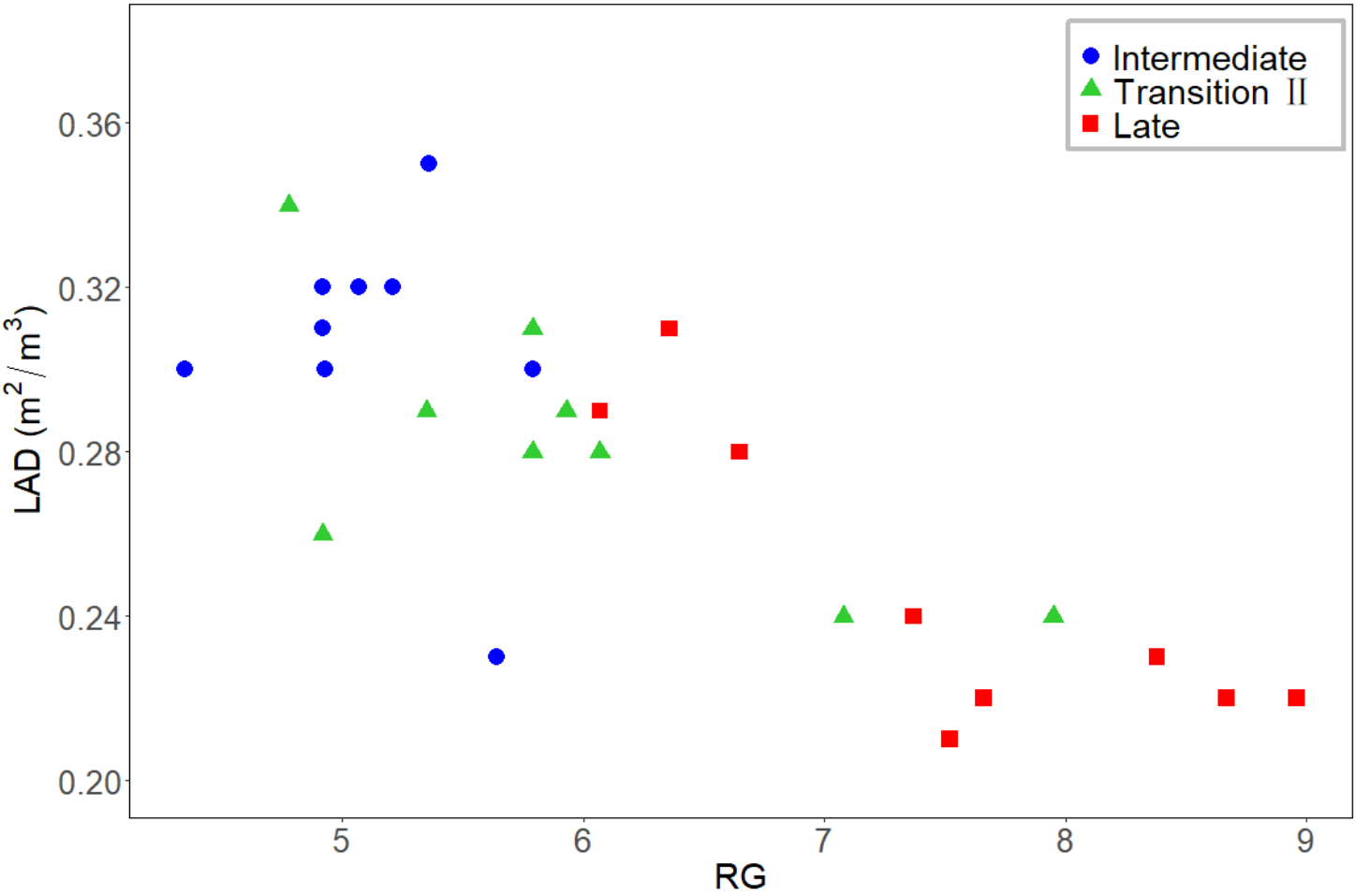

Figure 10. A scatter plot of RG (the radius of gyration) versus LAD (Leaf Area Density) from 27 plots distributed in three successional gradients (Intermediate, Transition II and Late) at the SRNP-EMSS, Guanacaste, Costa Rica.

3. Chapter 3: Conclusions

This research sought to advance the field of ecological succession by contributing to fill a gap in forest structure characterization for inter-successional stages (transitions) along the successional path. This was accomplished by first delineating canopy height changes between three principal successional stages and two transitions. The second objective was accomplished by deriving LAD vs Canopy Height profile and corresponding several shape-based metrics to characterize forest vertical structure variation in different successional stages and transitions.

3.1 Synthesis of significant contributions

As a result of forest fragmentation, the areas that include natural ecotones are constantly growing, therefore providing habitats for biodiversity, and protecting the interior of landscapes (Czaja et al., 2021). At the same time, these transitions play an important role in ecosystem regeneration and represent rich environments between successional stages. This study expands on previous studies by Li et al. (2017) and Sánchez-Azofeifa et al. (2017), who proposed mapping secondary TDFs succession should consider transitions between principal successional stages but did not characterize them.

The result of Chapter 2 “Characterizing transitions between successional stages in a Tropical Dry Forest site using LiDAR techniques” have detected transition zones at the SRNP-EMSS and characterized the forest structure along the successional path. Particularly, by characterizing forest structural variation, I have proposed the existence of transitions between principal successional stages and the importance to consider the TDFs regeneration as a continuous stochastic phenomenon. In other

words, the sequence of ecological regeneration evolve as Early – Transition I – Intermediate – Transition II – Late. Moreover, I have filled a knowledge gap regarding the forest structure features for transitions, which showed a unique difference compared with that of principal successional stages. Findings from this study highlighted the ecological significance of the transitions from early to intermediate successional stage and intermediate to late successional stage, which will contribute to understanding the significance of inter-successional stages (transitions) in TDFs. Finally, this work highlighted the advantages to incorporate LiDAR techniques to describe and quantify the TDFs regeneration.

3.2 Future work and challenge

One limitation of this study is that the canopy height and individual trees information for five successional stages may be underestimated because it was derived from a raster image (Canopy Height Model). That means abundant understory cannot be detected in the raster image, especially for trees in the transition II and the late successional stage with a big and dense canopy. Besides, due to the limitation of the data set, we could not characterize forest structure of lianas-infested forest patches or non-lianas transitions. Future studies can select lianas-infested plots of the transition in the field to assess the changes in tropical dry forest structure due to transitions and liana presence. The importance of this future work is because of lianas effects on ecosystem structure and composition, which in turn will affect faunal diversity, tree mortality, and carbon storage above and below ground (Schnitzer et al., 2014). However, this needs high-precision hyperspectral images or LiDAR data sets to detect lianas-infested plots in transition zones. Although, my study is limited to one single

site in Costa Rica this is the first step to exploring and under-standing forest structure characteristics of inter-successional stages (transitions).

3.3 References

Czaja, J., Wilczek, Z., Chmura, D., 2021. Shaping the ecotone zone in forest communities that are adjacent to expressway roads. Forests 12, 1–13. https://doi.org/10.3390/f12111490

Li, W., Cao, S., Campos-Vargas, C., Sanchez-Azofeifa, A., 2017. Identifying tropical dry forests extent and succession via the use of machine learning techniques. Int. J. Appl. Earth Obs. Geoinf. 63, 196–205. https://doi.org/10.1016/j.jag.2017.08.003

Sánchez-Azofeifa, G.A., Guzmán-Quesada, J.A., Vega-Araya, M., Campos-Vargas, C., Durán, S.M., D'Souza, N., Gianoli, T., Portillo-Quintero, C., Sharp, I., 2017. Can terrestrial laser scanners (TLSs) and hemispherical photographs predict tropical dry forest succession with liana abundance? Biogeosciences 14, 977–988. https://doi.org/10.5194/bg-14-977-2017

Schnitzer, S.A., Heijden, G. Van Der, Mascaro, J., Walter, P., Schnitzer, S.A., Heijden, G. Van Der, Mascaro, J., Carson, W.P., 2014. Lianas in gaps reduce carbon accumulation in a tropical forest Published by : Wiley on behalf of the Ecological Society of America Stable URL : http://www.jstor.org/stable/43495216 Lianas in gaps reduce carbon accumulation in a tropical forest. Ecology 95, 3008–3017. https://doi.org/https://doi.org/10.1890/13-1718.1

Bibliography

Chapter 1: Introduction

Abshire, J.B., Sun, X., Riris, H., Sirota, J.M., Mcgarry, J.F., Palm, S., Yi, D., Liiva, P., 2005. Geoscience Laser Altimeter System (GLAS) on the ICESat Mission : On-orbit measurement performance 32, 11–14. https://doi.org/10.1029/2005GL024028

Aide, M., Zimmerman, J., Rosario, M., Marcano, H., 1996. Forest Recovery in Abandoned Cattle Pastures Along an Elevational Gradient in Northeastern Puerto Rico Author (s): T . Mitchell Aide , Jess K . Zimmerman , Maydee Rosario and Humfredo Marcano Source : Biotropica , Vol . 28 , No . 4 , Part A . Special Is. Biotropica 28, 537–548.

Armston, J., Disney, M., Lewis, P., Scarth, P., Phinn, S., Lucas, R., Bunting, P., Goodwin, N., 2013. Remote Sensing of Environment Direct retrieval of canopy gap probability using airborne waveform lidar. Remote Sens. Environ. 134, 24–38. https://doi.org/10.1016/j.rse.2013.02.021

Arroyo-Mora, J.P., Sánchez-Azofeifa, G.A., Kalacska, M., Rivard, B., Calvo-Alvarado, J.C., Janzen, D.H., 2005. Secondary Forest Detection in a Neotropical Dry Forest Landscape Using Landsat 7 ETM + and IKONOS Imagery Published by : Association for Tropical Biology and Conservation Stable URL : https://www.jstor.org/stable/30043218 REFERENCES Linked references are. Biotropica 37, 497–507.

Bagaram, M.B., Giuliarelli, D., Chirici, G., Giannetti, F., Barbati, A., 2018. UAV remote sensing for biodiversity monitoring: Are forest canopy gaps good covariates? Remote Sens. 10, 1–28. https://doi.org/10.3390/rs10091397

Barbier, E.B., 2004. Agricultural expansion, resource booms and growth in Latin America: Implications for long-run economic development. World Dev. 32, 137–157. https://doi.org/10.1016/j.worlddev.2003.07.005

Blair, J.B., Rabine, D.L., Hofton, M.A., 1999. The Laser Vegetation Imaging Sensor : a medium-altitude , digitisation-only , airborne laser altimeter for mapping vegetation and topography 115–122.

Bottalico, F., Chirici, G., Giannini, R., Mele, S., Mura, M., Puxeddu, M., Mcroberts, R.E., Valbuena, R., Travaglini, D., 2017. International Journal of Applied Earth Observation and Geoinformation Modeling Mediterranean forest structure using airborne laser scanning data. Int. J. Appl. Earth Obs. Geoinf. 57, 145–153. https://doi.org/10.1016/j.jag.2016.12.013

Bouvier, M., Durrieu, S., Fournier, R.A., Renaud, J., 2015. Remote Sensing of Environment Generalizing predictive models of forest inventory attributes using an area-based approach with airborne LiDAR data. Remote Sens. Environ. 156, 322–334. https://doi.org/10.1016/j.rse.2014.10.004

Burrough, P.A., 2001. GIS and geostatistics: Essential partners for spatial analysis. Environ. Ecol. Stat. 8, 361–377. https://doi.org/10.1023/A:1012734519752

Calvo-Rodriguez, S., Sanchez-Azofeifa, A.G., Duran, S.M., Espírito-Santo, M.M., 2016. Assessing ecosystem services in Neotropical dry forests: A systematic review. Environ. Conserv. https://doi.org/10.1017/S0376892916000400

Cao, S., Yu, Q., Sanchez-Azofeifa, A., Feng, J., Rivard, B., Gu, Z., 2015. Mapping tropical dry forest succession using multiple criteria spectral mixture analysis. ISPRS J. Photogramm. Remote Sens. 109, 17–29. https://doi.org/10.1016/j.isprsjprs.2015.08.009

Castillo-Núñez, M., Sánchez-Azofeifa, G.A., Croitoru, A., Rivard, B., Calvo-Alvarado, J., Dubayah, R.O., 2011. Delineation of secondary succession mechanisms for tropical dry forests using LiDAR. Remote Sens. Environ. 115, 2217–2231. https://doi.org/10.1016/j.rse.2011.04.020

Castillo, M., Rivard, B., Sánchez-Azofeifa, A., Calvo-Alvarado, J., Dubayah, R., 2012. LIDAR remote sensing for secondary Tropical Dry Forest identification. Remote Sens. Environ. 121, 132–143. https://doi.org/10.1016/j.rse.2012.01.012

Clark, M.L., Clark, D.B., Roberts, D.A., 2004. Small-footprint lidar estimation of sub-canopy elevation and tree height in a tropical rain forest landscape. Remote Sens. Environ. 91, 68–89. https://doi.org/10.1016/j.rse.2004.02.008

Crespo-peremarch, P., Ángel, L., Balaguer-beser, Á., Estornell, J., Cartography, G., Sensing, R., Cgat, G., València, U.P. De, Vera, C. De, 2018. ISPRS Journal of Photogrammetry and Remote Sensing Analyzing the role of pulse density and voxelization parameters on full- waveform LiDAR-derived metrics. ISPRS J. Photogramm. Remote Sens. 146, 453–464. https://doi.org/10.1016/j.isprsjprs.2018.10.012

Crespo-Peremarch, P., Fournier, R.A., Nguyen, V.T., van Lier, O.R., Ruiz, L.Á., 2020. A comparative assessment of the vertical distribution of forest components using full-waveform airborne, discrete airborne and discrete terrestrial laser scanning data. For. Ecol. Manage. 473, 118268. https://doi.org/10.1016/j.foreco.2020.118268

Czaja, J., Wilczek, Z., Chmura, D., 2021. Shaping the ecotone zone in forest communities that are adjacent to expressway roads. Forests 12, 1–13. https://doi.org/10.3390/f12111490

Drake, J.B., Dubayah, R.O., Clark, D.B., Knox, R.G., Blair, J.B., Hofton, M.A., Chazdon, R.L., Weishampel, J.F., Prince, S.D., 2002. Estimation of tropical forest structural characteristics using large-footprint lidar. Remote Sens. Environ. 79, 305–319. https://doi.org/https://doi.org/10.1016/S0034-4257(01)00281-4

Gentry, A., 1988. Volume 75 Annals Number 1 of the Botanical Garden. Ann. Missouri Bot. Gard. 75, 1–34.

Gu, Z., Cao, S., Sanchez-Azofeifa, G.A., 2018. Using LiDAR waveform metrics to describe and identify successional stages of tropical dry forests. Int. J. Appl. Earth Obs. Geoinf. 73, 482–492. https://doi.org/10.1016/j.jag.2018.07.010

Hoekstra, J.M., Boucher, T.M., Ricketts, T.H., Roberts, C., 2005. Confronting a biome crisis: Global disparities of habitat loss and protection. Ecol. Lett. 8, 23–29. https://doi.org/10.1111/j.1461-0248.2004.00686.x

Houghton, R.A., Skole, D.L., Lefkowitz, D.S., 1991. Changes in the landscape of Latin America between 1850 and 1985 II. Net release of CO2 to the atmosphere. For. Ecol. Manage. 38, 173–199. https://doi.org/10.1016/0378-1127(91)90141-H

Janzen, D.H., 1986. The Future of Tropical Ecology Author (s): Daniel H . Janzen Source : Annual Review of Ecology and Systematics , Vol . 17 (1986), pp . 305-324 Published by : Annual Reviews Stable URL : http://www.jstor.org/stable/2096998 THE FUTURE OF TROPICAL ECOLOG. For. Ecol. Manage. 17, 305–324.

Kalácska, M., Calvo-Alvarado, J.C., Sánchez-Azofeifa, G.A., 2005. Calibration and assessment of seasonal changes in leaf area index of a tropical dry forest in different stages of succession. Tree Physiol. 25, 733–744. https://doi.org/10.1093/treephys/25.6.733

Kalacska, M., Member, S., Sanchez-azofeifa, G.A., Caelli, T., Rivard, B., Boerlage, B., 2005. Using Bayesian Networks. IEEE Trans. Geosci. Remote Sens. 43, 1866–1873. https://doi.org/https://doi.org/10.1109/TGRS.2005.848412

Kalacska, M., Sanchez-Azofeifa, G.A., Calvo-Alvarado, J.C., Quesada, M., Rivard, B., Janzen, D.H., 2004. Species composition, similarity and diversity in three successional stages of a seasonally dry tropical forest. For. Ecol. Manage. 200, 227–247. https://doi.org/10.1016/j.foreco.2004.07.001

Kalacska, M., Sanchez-azofeifa, G.A., Rivard, B., Caelli, T., 2007. Ecological fingerprinting of ecosystem succession : Estimating secondary tropical dry forest structure and diversity using imaging spectroscopy. Remote Sens. Environ. 108, 82–96. https://doi.org/10.1016/j.rse.2006.11.007

Khurana, E., Singh, J.S., 2001. Ecology of seed and seedling growth for conservation and restoration of tropical dry forest : A review. Environ. Conserv. 28, 39–52. https://doi.org/10.1017/S0376892901000042

Latifi, H., 2009. Characterizing Forest Structure by Means of Remote Sensing : A Review.

Leafsky, M.A.., Cohen, W.B.., Parker, G.G.., Harding, D.J., 2002. Lidar Remote Sensing for Ecosystem Studies. Bioscience 52, 19–30.

https://doi.org/https://doi.org/10.1641/0006-3568(2002)052[0019:LRSFES]2.0.CO;2

Li, W., Cao, S., Campos-Vargas, C., Sanchez-Azofeifa, A., 2017. Identifying tropical dry forests extent and succession via the use of machine learning techniques. Int. J. Appl. Earth Obs. Geoinf. 63, 196–205. https://doi.org/10.1016/j.jag.2017.08.003

Lovell, J.L., Jupp, D.L.B., Culvenor, D.S., Coops, N.C., 2003. Using airborne and ground-based ranging lidar to measure canopy structure in Australian forests. Can. J. Remote Sens. 29, 607–622. https://doi.org/10.5589/m03-026

Mallet, C., Bretar, F., 2009. ISPRS Journal of Photogrammetry and Remote Sensing Full-waveform topographic lidar : State-of-the-art. ISPRS J. Photogramm. Remote Sens. 64, 1–16. https://doi.org/10.1016/j.isprsjprs.2008.09.007

Marquette, C.M., 2006. Settler welfare on tropical forest frontiers in Latin America. Popul. Environ. 27, 397–444. https://doi.org/10.1007/s11111-006-0029-y

Martínez-Garza, C., González-Montagut, R., 1999. Seed rain from forest fragments into tropical pastures in Los Tuxtlas, Mexico. Plant Ecol. 145, 255–265. https://doi.org/10.1023/A:1009879505765

Meeussen, C., Govaert, S., Vanneste, T., Calders, K., Bollmann, K., Brunet, J., Cousins, S.A.O., Diekmann, M., Graae, B.J., Hedwall, P.O., Krishna Moorthy, S.M., Iacopetti, G., Lenoir, J., Lindmo, S., Orczewska, A., Ponette, Q., Plue, J., Selvi, F., Spicher, F., Tolosano, M., Verbeeck, H., Verheyen, K., Vangansbeke, P., De Frenne, P., 2020. Structural variation of forest edges across Europe. For. Ecol. Manage. 462, 117929. https://doi.org/10.1016/j.foreco.2020.117929

Muss, J.D., Aguilar-amuchastegui, N., Mladenoff, D.J., Henebry, G.M., 2013. Analysis of Waveform Lidar Data Using Shape-Based Metrics. IEEE Geosci. Remote Sens. Lett. 10, 106–110. https://doi.org/https://doi.org/10.1109/LGRS.2012.2194472

Novotný, J., Navrátilová, B., Janoutová, R., Oulehle, F., Homolová, L., 2020. Influence of site-specific conditions on estimation of forest above ground biomass from airborne laser scanning. Forests 11, 1–18. https://doi.org/10.3390/f11030268

Olson, D.M., Dinerstein, E., Wikramanayake, E.D., Burgess, N.D., Powell, G.V.N., Underwood, E.C., Amico, J.A.D., Itoua, I., Strand, H.E., Morrison, J.C., Loucks,

J., Allnutt, T.F., Ricketts, T.H., Kura, Y., Lamoreux, J.F., Wesley, W., Hedao, P., Kassem, K.R., 2001. Terrestrial Ecoregions of the World : A New Map of Life on Earth 51, 933–938.

Portillo-Quintero, C.A., Sánchez-Azofeifa, G.A., 2010. Extent and conservation of tropical dry forests in the Americas. Biol. Conserv. 143, 144–155. https://doi.org/10.1016/j.biocon.2009.09.020

Quesada, M., Sanchez-Azofeifa, G.A., Alvarez-Añorve, M., Stoner, K.E., Avila-Cabadilla, L., Calvo-Alvarado, J., Castillo, A., Espírito-Santo, M.M., Fagundes, M., Fernandes, G.W., Gamon, J., Lopezaraiza-Mikel, M., Lawrence, D., Morellato, L.P.C., Powers, J.S., Neves, F. de S., Rosas-Guerrero, V., Sayago, R., Sanchez-Montoya, G., 2009. Succession and management of tropical dry forests in the Americas: Review and new perspectives. For. Ecol. Manage. 258, 1014–1024. https://doi.org/10.1016/j.foreco.2009.06.023

Ruiz, L.A., Hermosilla, T., Mauro, F., Godino, M., 2014. Analysis of the Influence of Plot Size and LiDAR Density on Forest Structure Attribute Estimates. Forests 936–951. https://doi.org/10.3390/f5050936

Sánchez-Azofeifa, G.A., Guzmán-Quesada, J.A., Vega-Araya, M., Campos-Vargas, C., Durán, S.M., D'Souza, N., Gianoli, T., Portillo-Quintero, C., Sharp, I., 2017. Can terrestrial laser scanners (TLSs) and hemispherical photographs predict tropical dry forest succession with liana abundance? Biogeosciences 14, 977–988. https://doi.org/10.5194/bg-14-977-2017

Sánchez-Azofeifa, G.A., Quesada, M., Rodríguez, J.P., Jafet, M., Stoner, K.E., Castillo, A., Garvin, T., Zent, Egleé L, Calvo-, J.C., Kalacska, M.E.R., Fajardo, L., Gamon, J.A., Cuevas-, P., Sanchez-azofeifa, G.A., Quesada, M., Rodriguez, J.P., Nassar, J.M., Stoner, K.E., Castillo, A., Garvin, T., Zent, Eglee L, Calvo-alvarado, J.C., Kalacska, M.E.R., Fajardo, L., Gamon, J.A., Forestal, D.I., Manejo, P. De, Recursos, C. De, Rica, I.T.D.C., 2005. Research Priorities for Neotropical Dry Forests Published by : Association for Tropical Biology and Conservation Stable URL : https://www.jstor.org/stable/30043216 Research Priorities for Neotropical Dry Forests '. Biotropica.

Schnitzer, S.A., Heijden, G. Van Der, Mascaro, J., Walter, P., Schnitzer, S.A., Heijden, G. Van Der, Mascaro, J., Carson, W.P., 2014. Lianas in gaps reduce carbon accumulation in a tropical forest Published by : Wiley on behalf of the Ecological Society of America Stable URL : http://www.jstor.org/stable/43495216 Lianas in gaps reduce carbon accumulation in a tropical forest. Ecology 95, 3008–3017. https://doi.org/https://doi.org/10.1890/13-1718.1

Skowronski, N.S., Clark, K.L., Gallagher, M., Birdsey, R.A., Hom, J.L., 2014. Airborne laser scanner-assisted estimation of aboveground biomass change in a temperate oak-pine forest. Remote Sens. Environ. 151, 166–174. https://doi.org/10.1016/j.rse.2013.12.015

Zhao, G., Sanchez-azofeifa, A., Laakso, K., Sun, C., Fei, L., 2021. Hyperspectral and Full-Waveform LiDAR Improve Mapping of Tropical Dry Forest ' s Successional Stages. Remote Sens. https://doi.org/https://doi.org/10.3390/rs13193830

Zhao, K., Popescu, S., Nelson, R., 2009. Lidar remote sensing of forest biomass: A scale-invariant estimation approach using airborne lasers. Remote Sens. Environ. 113, 182–196. https://doi.org/10.1016/j.rse.2008.09.009

Chapter 2: Characterizing Transitions between successional stages in a Tropical Dry Forest using LiDAR Techniques

Arroyo-Mora, J.P., Sánchez-Azofeifa, G.A., Kalacska, M., Rivard, B., Calvo-Alvarado, J.C., Janzen, D.H., 2005. Secondary Forest Detection in a Neotropical Dry Forest Landscape Using Landsat 7 ETM + and IKONOS Imagery Published by : Association for Tropical Biology and Conservation Stable URL : https://www.jstor.org/stable/30043218 REFERENCES Linked references are. Biotropica 37, 497–507.

Bagaram, M.B., Giuliarelli, D., Chirici, G., Giannetti, F., Barbati, A., 2018. UAV remote sensing for biodiversity monitoring: Are forest canopy gaps good covariates? Remote Sens. 10, 1–28. https://doi.org/10.3390/rs10091397

Bottalico, F., Chirici, G., Giannini, R., Mele, S., Mura, M., Puxeddu, M., Mcroberts, R.E., Valbuena, R., Travaglini, D., 2017. International Journal of Applied Earth Observation and Geoinformation Modeling Mediterranean forest structure using

airborne laser scanning data. Int. J. Appl. Earth Obs. Geoinf. 57, 145–153. https://doi.org/10.1016/j.jag.2016.12.013

Bouvier, M., Durrieu, S., Fournier, R.A., Renaud, J., 2015. Remote Sensing of Environment Generalizing predictive models of forest inventory attributes using an area-based approach with airborne LiDAR data. Remote Sens. Environ. 156, 322–334. https://doi.org/10.1016/j.rse.2014.10.004

Bréda, N.J.J., 2003. Ground-based measurements of leaf area index: A review of methods, instruments and current controversies. J. Exp. Bot. 54, 2403–2417. https://doi.org/10.1093/jxb/erg263

Burrough, P.A., 2001. GIS and geostatistics: Essential partners for spatial analysis. Environ. Ecol. Stat. 8, 361–377. https://doi.org/10.1023/A:1012734519752

Calvo-Rodriguez, S., Sanchez-Azofeifa, A.G., Duran, S.M., Espírito-Santo, M.M., 2016. Assessing ecosystem services in Neotropical dry forests: A systematic review. Environ. Conserv. https://doi.org/10.1017/S0376892916000400

Calvo-Rodriguez, S., Sánchez-Azofeifa, G.A., Durán, S.M., Espírito-Santo, M.M. Do, Nunes, Y.R.F., 2021. Dynamics of carbon accumulation in tropical dry forests under climate change extremes. Forests 12, 1–15. https://doi.org/10.3390/f12010106

Cao, S., Sanchez-Azofeifa, G.A., Duran, S.M., Calvo-Rodriguez, S., 2016. Estimation of aboveground net primary productivity in secondary tropical dry forests using the Carnegie-Ames-Stanford approach (CASA) model. Environ. Res. Lett. 11. https://doi.org/10.1088/1748-9326/11/7/075004

Cao, S., Yu, Q., Sanchez-Azofeifa, A., Feng, J., Rivard, B., Gu, Z., 2015. Mapping tropical dry forest succession using multiple criteria spectral mixture analysis. ISPRS J. Photogramm. Remote Sens. 109, 17–29. https://doi.org/10.1016/j.isprsjprs.2015.08.009

Castillo-Núñez, M., Sánchez-Azofeifa, G.A., Croitoru, A., Rivard, B., Calvo-Alvarado, J., Dubayah, R.O., 2011. Delineation of secondary succession mechanisms for tropical dry forests using LiDAR. Remote Sens. Environ. 115, 2217–2231. https://doi.org/10.1016/j.rse.2011.04.020

Castillo, M., Rivard, B., Sánchez-Azofeifa, A., Calvo-Alvarado, J., Dubayah, R., 2012. LIDAR remote sensing for secondary Tropical Dry Forest identification. Remote Sens. Environ. 121, 132–143. https://doi.org/10.1016/j.rse.2012.01.012

Chaulagain, S., Stone, M.C., Dombroski, D., Gillihan, T., Chen, L., Zhang, S., 2022. An investigation into remote sensing techniques and field observations to model hydraulic roughness from riparian vegetation. River Res. Appl. 1730–1745. https://doi.org/10.1002/rra.4053

Clark, M.L., Clark, D.B., Roberts, D.A., 2004. Small-footprint lidar estimation of sub-canopy elevation and tree height in a tropical rain forest landscape. Remote Sens. Environ. 91, 68–89. https://doi.org/10.1016/j.rse.2004.02.008

Crespo-peremarch, P., Ángel, L., Balaguer-beser, Á., Estornell, J., Cartography, G., Sensing, R., Cgat, G., València, U.P. De, Vera, C. De, 2018. ISPRS Journal of Photogrammetry and Remote Sensing Analyzing the role of pulse density and voxelization parameters on full- waveform LiDAR-derived metrics. ISPRS J. Photogramm. Remote Sens. 146, 453–464. https://doi.org/10.1016/j.isprsjprs.2018.10.012

Crespo-Peremarch, P., Fournier, R.A., Nguyen, V.T., van Lier, O.R., Ruiz, L.Á., 2020. A comparative assessment of the vertical distribution of forest components using full-waveform airborne, discrete airborne and discrete terrestrial laser scanning data. For. Ecol. Manage. 473, 118268. https://doi.org/10.1016/j.foreco.2020.118268

de Almeida, D.R.A., Stark, S.C., Shao, G., Schietti, J., Nelson, B.W., Silva, C.A., Gorgens, E.B., Valbuena, R., Papa, D. de A., Brancalion, P.H.S., 2019. Optimizing the remote detection of tropical rainforest structure with airborne lidar: Leaf area profile sensitivity to pulse density and spatial sampling. Remote Sens. 11. https://doi.org/10.3390/rs11010092

Drake, J.B., Dubayah, R.O., Clark, D.B., Knox, R.G., Blair, J.B., Hofton, M.A., Chazdon, R.L., Weishampel, J.F., Prince, S.D., 2002. Estimation of tropical forest structural characteristics using large-footprint lidar. Remote Sens. Environ. 79, 305–319. https://doi.org/https://doi.org/10.1016/S0034-4257(01)00281-4

Gu, Z., Cao, S., Sanchez-Azofeifa, G.A., 2018. Using LiDAR waveform metrics to describe and identify successional stages of tropical dry forests. Int. J. Appl. Earth Obs. Geoinf. 73, 482–492. https://doi.org/10.1016/j.jag.2018.07.010

Han, T., Sánchez-azofeifa, G.A., 2022. Extraction of Liana Stems Using Geometric Features from Terrestrial Laser Scanning Point Clouds. Remote Sens. https://doi.org/https://doi.org/10.3390/rs14164039

Hoekstra, J.M., Boucher, T.M., Ricketts, T.H., Roberts, C., 2005. Confronting a biome crisis: Global disparities of habitat loss and protection. Ecol. Lett. 8, 23–29. https://doi.org/10.1111/j.1461-0248.2004.00686.x

Ingwell, L.L., Joseph Wright, S., Becklund, K.K., Hubbell, S.P., Schnitzer, S.A., 2010. The impact of lianas on 10 years of tree growth and mortality on Barro Colorado Island, Panama. J. Ecol. 98, 879–887. https://doi.org/10.1111/j.1365-2745.2010.01676.x

Isenburg, M., Liu, Y., Shewchuk, J., Snoeyink, J., 2006a. Streaming computation of delaunay triangulations. ACM Trans. Graph. 25, 1049–1056. https://doi.org/10.1145/1141911.1141992

Isenburg, M., Liu, Y., Shewchuk, J., Snoeyink, J., Thirion, T., 2006b. Generating raster DEM from mass points via TIN streaming. Lect. Notes Comput. Sci. (including Subser. Lect. Notes Artif. Intell. Lect. Notes Bioinformatics) 4197 LNCS, 186–198. https://doi.org/10.1007/11863939_13

Janzen, D.H., 1986. The Future of Tropical Ecology Author (s): Daniel H . Janzen Source : Annual Review of Ecology and Systematics , Vol . 17 (1986), pp . 305-324 Published by : Annual Reviews Stable URL : http://www.jstor.org/stable/2096998 THE FUTURE OF TROPICAL ECOLOG. For. Ecol. Manage. 17, 305–324.

Kalácska, M., Calvo-Alvarado, J.C., Sánchez-Azofeifa, G.A., 2005. Calibration and assessment of seasonal changes in leaf area index of a tropical dry forest in different stages of succession. Tree Physiol. 25, 733–744. https://doi.org/10.1093/treephys/25.6.733

Kalacska, M., Member, S., Sanchez-azofeifa, G.A., Caelli, T., Rivard, B., Boerlage, B., 2005. Using Bayesian Networks. IEEE Trans. Geosci. Remote Sens. 43, 1866–1873. https://doi.org/https://doi.org/10.1109/TGRS.2005.848412

Kalacska, M., Sanchez-Azofeifa, G.A., Calvo-Alvarado, J.C., Quesada, M., Rivard, B., Janzen, D.H., 2004. Species composition, similarity and diversity in three successional stages of a seasonally dry tropical forest. For. Ecol. Manage. 200, 227–247. https://doi.org/10.1016/j.foreco.2004.07.001

Kalacska, M., Sanchez-azofeifa, G.A., Rivard, B., Caelli, T., 2007. Ecological fingerprinting of ecosystem succession : Estimating secondary tropical dry forest structure and diversity using imaging spectroscopy. Remote Sens. Environ. 108, 82–96. https://doi.org/10.1016/j.rse.2006.11.007

Laurance, W.F., Lovejoy, T.E., Vasconcelos, H.L., Bruna, E.M., Didham, R.K., Stouffer, P.C., Gascon, C., Bierregaard, R.O., Laurance, S.G., Sampaio, E., 2002. Ecosystem Decay of Amazonian Forest Fragments : a 22-Year Investigation. Ecosyst. Decay Amaz. Fragm. 16, 605–618.

Leafsky, M.A.., Cohen, W.B.., Parker, G.G.., Harding, D.J., 2002. Lidar Remote Sensing for Ecosystem Studies. Bioscience 52, 19–30. https://doi.org/https://doi.org/10.1641/0006-3568(2002)052[0019:LRSFES]2.0.CO;2

Li, W., Cao, S., Campos-Vargas, C., Sanchez-Azofeifa, A., 2017. Identifying tropical dry forests extent and succession via the use of machine learning techniques. Int. J. Appl. Earth Obs. Geoinf. 63, 196–205. https://doi.org/10.1016/j.jag.2017.08.003

Manu, S., Peach, W., Cresswell, W., 2007. The effects of edge , fragment size and degree of isolation on avian species richness in highly fragmented forest in West Africa 287–297.

Martens, S.N., Ustin, S.L., Rousseau, R.A., 1993. Estimation of tree canopy leaf area index by gap fraction analysis. For. Ecol. Manage. 61, 91–108. https://doi.org/10.1016/0378-1127(93)90192-P

Martínez-Garza, C., González-Montagut, R., 1999. Seed rain from forest fragments into tropical pastures in Los Tuxtlas, Mexico. Plant Ecol. 145, 255–265. https://doi.org/10.1023/A:1009879505765

Muss, J.D., Aguilar-amuchastegui, N., Mladenoff, D.J., Henebry, G.M., 2013. Analysis of Waveform Lidar Data Using Shape-Based Metrics. IEEE Geosci. Remote Sens. Lett. 10, 106–110. https://doi.org/https://doi.org/10.1109/LGRS.2012.2194472

Novotný, J., Navrátilová, B., Janoutová, R., Oulehle, F., Homolová, L., 2020. Influence of site-specific conditions on estimation of forest above ground biomass from airborne laser scanning. Forests 11, 1–18. https://doi.org/10.3390/f11030268

Paul, G.S., Yavitt, J.B., 2011. Tropical Vine Growth and the Effects on Forest Succession: A Review of the Ecology and Management of Tropical Climbing Plants. Bot. Rev. 77, 11–30. https://doi.org/10.1007/s12229-010-9059-3

Portillo-quintero, C., Sánchez-azofeifa, A., Espírito-santo, M.M., 2013. Edge Influence on Canopy Openness and Understory Microclimate in Two Neotropical Dry Forest Fragments 157–172.

Portillo-Quintero, C.A., Sánchez-Azofeifa, G.A., 2010. Extent and conservation of tropical dry forests in the Americas. Biol. Conserv. 143, 144–155. https://doi.org/10.1016/j.biocon.2009.09.020

Quesada, M., Sanchez-Azofeifa, G.A., Alvarez-Añorve, M., Stoner, K.E., Avila-Cabadilla, L., Calvo-Alvarado, J., Castillo, A., Espírito-Santo, M.M., Fagundes, M., Fernandes, G.W., Gamon, J., Lopezaraiza-Mikel, M., Lawrence, D., Morellato, L.P.C., Powers, J.S., Neves, F. de S., Rosas-Guerrero, V., Sayago, R., Sanchez-Montoya, G., 2009. Succession and management of tropical dry forests in the Americas: Review and new perspectives. For. Ecol. Manage. 258, 1014–1024. https://doi.org/10.1016/j.foreco.2009.06.023

Rodríguez-Ronderos, M.E., Bohrer, G., Sanchez-Azofeifa, A., Powers, J.S., Schnitzer, S.A., 2016. Contribution of lianas to plant area index and canopy structure in a Panamanian forest. Ecology 97, 3271–3277. https://doi.org/10.1002/ecy.1597

Ruiz, L.A., Hermosilla, T., Mauro, F., Godino, M., 2014. Analysis of the Influence of Plot Size and LiDAR Density on Forest Structure Attribute Estimates. Forests 936–951. https://doi.org/10.3390/f5050936

Sánchez-Azofeifa, G.A., Guzmán-Quesada, J.A., Vega-Araya, M., Campos-Vargas, C., Durán, S.M., D'Souza, N., Gianoli, T., Portillo-Quintero, C., Sharp, I., 2017. Can terrestrial laser scanners (TLSs) and hemispherical photographs predict tropical

dry forest succession with liana abundance? Biogeosciences 14, 977–988. https://doi.org/10.5194/bg-14-977-2017

Sánchez-Azofeifa, G.A., Quesada, M., Rodríguez, J.P., Jafet, M., Stoner, K.E., Castillo, A., Garvin, T., Zent, Egleé L, Calvo-, J.C., Kalacska, M.E.R., Fajardo, L., Gamon, J.A., Cuevas-, P., Sanchez-azofeifa, G.A., Quesada, M., Rodriguez, J.P., Nassar, J.M., Stoner, K.E., Castillo, A., Garvin, T., Zent, Eglee L, Calvo-alvarado, J.C., Kalacska, M.E.R., Fajardo, L., Gamon, J.A., Forestal, D.I., Manejo, P. De, Recursos, C. De, Rica, I.T.D.C., 2005. Research Priorities for Neotropical Dry Forests Published by : Association for Tropical Biology and Conservation Stable URL : https://www.jstor.org/stable/30043216 Research Priorities for Neotropical Dry Forests '. Biotropica.

Schnitzer, S.A., 2005. A mechanistic explanation for global patterns of liana abundance and distribution. Am. Nat. 166, 262–276. https://doi.org/10.1086/431250

Schnitzer, S.A., Heijden, G. Van Der, Mascaro, J., Walter, P., Schnitzer, S.A., Heijden, G. Van Der, Mascaro, J., Carson, W.P., 2014. Lianas in gaps reduce carbon accumulation in a tropical forest Published by : Wiley on behalf of the Ecological Society of America Stable URL : http://www.jstor.org/stable/43495216 Lianas in gaps reduce carbon accumulation in a tropical forest. Ecology 95, 3008–3017. https://doi.org/https://doi.org/10.1890/13-1718.1

Smith, P.R., 1981. Bilinear interpolation of digital images. Ultramicroscopy 6, 201–204. https://doi.org/10.1016/S0304-3991(81)80199-4

Vose, J.M., Sullivan, N.H., Clinton, B.D., Bolstad, P. V., 1995. Vertical leaf area distribution, light transmittance, and application of the Beer-Lambert Law in four mature hardwood stands in the southern Appalachians. Can. J. For. Res. 25, 1036–1043. https://doi.org/10.1139/x95-113

Zhang, W., Qi, J., Wan, P., Wang, H., Xie, D., Wang, X., Yan, G., 2016. An easy-to-use airborne LiDAR data filtering method based on cloth simulation. Remote Sens. 8, 1–22. https://doi.org/10.3390/rs8060501

Zhao, G., Sanchez-azofeifa, A., Laakso, K., Sun, C., Fei, L., 2021. Hyperspectral and Full-Waveform LiDAR Improve Mapping of Tropical Dry Forest' s Successional Stages. Remote Sens. https://doi.org/https://doi.org/10.3390/rs13193830

Chapter 3: Conclusions

Czaja, J., Wilczek, Z., Chmura, D., 2021. Shaping the ecotone zone in forest communities that are adjacent to expressway roads. Forests 12, 1–13. https://doi.org/10.3390/f12111490

Li, W., Cao, S., Campos-Vargas, C., Sanchez-Azofeifa, A., 2017. Identifying tropical dry forests extent and succession via the use of machine learning techniques. Int. J. Appl. Earth Obs. Geoinf. 63, 196–205. https://doi.org/10.1016/j.jag.2017.08.003

Sánchez-Azofeifa, G.A., Guzmán-Quesada, J.A., Vega-Araya, M., Campos-Vargas, C., Durán, S.M., D'Souza, N., Gianoli, T., Portillo-Quintero, C., Sharp, I., 2017. Can terrestrial laser scanners (TLSs) and hemispherical photographs predict tropical dry forest succession with liana abundance? Biogeosciences 14, 977–988. https://doi.org/10.5194/bg-14-977-2017

Schnitzer, S.A., Heijden, G. Van Der, Mascaro, J., Walter, P., Schnitzer, S.A., Heijden, G. Van Der, Mascaro, J., Carson, W.P., 2014. Lianas in gaps reduce carbon accumulation in a tropical forest Published by : Wiley on behalf of the Ecological Society of America Stable URL : http://www.jstor.org/stable/43495216 Lianas in gaps reduce carbon accumulation in a tropical forest. Ecology 95, 3008–3017. https://doi.org/https://doi.org/10.1890/13-1718.1